Available online at www.sciencedirect.com
SCIENCE DIRECT
International Journal of Mass Spectrometry 246 (2005) 84–104
International Journal of Mass Spectrometry
www.elsevier.com/locate/ijms

Investigation of chemical reactions in solution using API-MS

Leonardo Silva Santos, Larissa Knaack, Jürgen O. Metzger *

Institut für Reine und Angewandte Chemie, Carl von Ossietzky Universität, 26111 Oldenburg, Germany

Received 19 May 2005; received in revised form 19 August 2005; accepted 22 August 2005
Available online 22 September 2005

Abstract

The general concepts, advantages, and applications of on-line and off-line screening to organic reaction mechanistic studies applying API-MS are reviewed. An overview is presented of the development and the present stage of connected microreactors to API ion-sources. Examples of the successful application of API in revealing, elucidating, and helping to consolidate several proposed mechanisms of organic reactions are summarized. Finally, a variety of outstanding features and advantages that make API-MS the most suitable tool for the fast screening of intermediates directly from solution, and the exceptional gains in chemical information for organic chemists are also emphasized.

Keywords: Reaction mechanism; ESI-MS; APCI-MS; Microreactor; On-line screening

1. Introduction

The recent developments of mass spectrometric ionization methods at atmospheric pressure (API) like electrospray ionization (ESI) [1], atmospheric pressure chemical ionization (APCI) [2], thermospray ionization (TI), and atmospheric pressure photo ionization (APPI) [3], enable the investigation of liquid solutions by mass spectrometry. These ionization methods opened up the access to the direct investigation of chemical reactions in solution via mass spectrometry. In principle, these methods make possible the detection and study not only of reaction substrates and products, but even short-lived reaction intermediates as they are present in solution, providing new insights of the mechanism of the reactions studied.

ESI-MS and its tandem version ESI-MS/MS are rapidly becoming the techniques of choice for solution mechanistic studies in chemistry and biochemistry, and in high-throughput screening of homogeneous catalysis reactions [4]. The principal outcome of the ESI process is the transfer of analyte species generally ionized in the condensed phase into the gas phase as isolated entities. One of the most interesting methodologies using ESI is the "ion-fishing" technique [5]. The suspected catalytic ionic species is "fished" from solution and transfered to the collision cell of the mass spectrometer, where the gas phase catalytic reaction is studied. For example, Chen and co-workers used this technique to study important homogeneously transition metal catalyzed reactions. However, this important methodology has been recently reviewed [6] and will not be discussed in this paper.

In general, ESI is used for ionic species in solution. However, for neutral molecules not easily protonated in solution, and not too labile, atmospheric pressure chemical ionization (APCI) is the best tool. APCI and ESI are the most utilized API methods for coupling liquid-phase to mass spectrometers. They are complementary in nature in that APCI is generally better suited for less polar species than ESI. Analogous to the chemical ionization, APCI is a relatively soft ionization and induces little or even no fragmentation of the analyte. A brief comment in the mechanism is taken to distinguish APCI from ESI. No voltages are applied in the spray formation in APCI, the neutral molecules are carried to the gas phase by a thermic process. The desolvation process is reached by heating the solution within the APCI assembly, normally maintained between 150 and 550 °C. A corona discharge needle with an applied voltage between 3000 and 5000 V provides electrons that ionize the gaseous analyte via a series of gas phase ion/molecule reactions at atmospheric pressure. In the positive ion mode, for instance, the energetic electrons initiate a sequence of reactions with the nebulizing gas (typically nitrogen) giving rise to nitrogen molecular ions. Depending on the composition of the mobile phase (solvent, S), ions such as $S^{\bullet+}$, $[S + H]^+$, and others are formed via a series of ion/molecule reactions with the nitrogen molecular ions. The ionization is

* Corresponding author. Tel.: +49 441 7983718; fax: +49 441 7983329.
E-mail address: juergen.metzger@uni-oldenburg.de (J.O. Metzger).

1387-3806/$ – see front matter © 2005 Elsevier B.V. All rights reserved.
doi:10.1016/j.ijms.2005.08.016

therefore initiated by electron transfer to the radical cation $S^{\bullet+}$ and by exothermic proton transfers from the protonated solvent ion. The neutral analyte molecules are consequently yielded in the gas phase into the radical and the protonated molecular ion, respectively [7].

This review deals with the use of API-MS in the organic reaction mechanistic studies in the condensed phase. We focus on the interception of intermediates in organic reactions previously proposed based on experimental evidences, and isolation of the different products, validating or not the empiric proposals. The relevant literature up to 2004 has been covered. However, kinetic studies using ESI-MS [8] as well as on-line coupling of electrochemistry with mass spectrometry [9] were reviewed quite recently and therefore will not be considered.

More detailed information can be found in some excellent reviews that summarize the current thinking on the several stages of the ESI process [10,11]. However, a brief comment in the mechanism must be emphasized.

The course of the electrospray process can be described with relative simplicity. A solution of the analyte is passed through a capillary hold at high potential. The high voltage generates a mist of highly charged droplets which passes through a potential and pressure gradient towards the analyzer portion of the mass spectrometer. During that transition, the droplets reduce their size by evaporation of the solvent and by droplet subdivision resulting from the coulombic repulsions caused by the high charge density achieved in the shrinkage. As final result, the ions become completely desolvated [12].

The charge state of the isolated ions is expected to closely reflect the charge state in solution [13], since the transfer of ions to the gas phase is not an energetic process—the desolvation is indeed a process that effectively cools the ions [14]. Therefore, it can be assumed that the ESI involves only the stepwise disruption of non-covalent interactions, principally the removal of molecules of solvation [15]. For example, in a detailed study by Kebarle and Ho, the transfer to the gas phase of different ions dissolved in a wide variety of solvents [16] was possible by ESI. It included singly and multiply charged inorganic ions, e.g., alkali, alkaline earths, and transition metals, organometallic species, and singly and multiply protonated or deprotonated organic compounds, e.g., amines, peptides, proteins, carboxylic acids, and nucleic acids.

The experimental information available so far on the preservation of the charge is not clarifying [17]. Single-electron transfer can occur during the electrospray process, because the ESI capillary may act as an electrolytic half-cell. Many neutral molecules, i.e., porphyrins, polycyclic aromatic hydrocarbons, aromatic amines, heteroaromatics, and metallocenes with low redox potentials are oxidized to form radical cations, allowing their detection in the gas phase. Analytes with redox potentials less than about 0.3 V vs. SCE were found to be almost completely oxidized by this process and detected at low levels [18]. However, the efficiency of oxidation detection decreased dramatically for analytes with redox potentials greater than 0.3 V. In the negative ion mode, the reduction of some neutrals, i.e., quinones, fullerene to form radical anions has been reported.

There are some documented cases where the charge state is changed after the desolvation process, like the multiply charged inorganic and organic ions, which are sometimes not seen in their expected charge state. The change occurs mainly for ions with the charge localized on one single atom or small group of them, e.g., M^{z+} with $z>1$; SO_4^{2-}, PO_4^{3-} [19]. When the multiple charge is confined to such a small volume, the high coulombic repulsions present forces the ion to undergo a charge reduction by intra-cluster proton transfer reaction in case of protic solvents, or by charge separation between the metal center and the bonded solvent molecules when aprotic solvents are used. Such reduction processes are promoted by collisions with residual gas molecules in the source interface region [20]. The interception of multiply charged naked ions can be achieved when the charge is stabilized by solvent molecules or ligands.

The intensity of the detected gas phase ions and the corresponding concentrations of these ions in the electrosprayed solution is related. However, in cases where the solution contains compounds able to react with these ions, the intensities may change drastically and much more complex relationships may prevail. As an example, some protonated bases and deprotonated acids can afford unexpected proton-transfer chemistry. This donation is associated with unusual conditions prevailing in the ion transfer process from the droplet to the gas phase, since solution and gas phase are two different environments for ionic species.

The coordination properties of supramolecular compounds may also differ between the solution and the gas phase. It is well known that polydentate ligands capable of forming stable solution complexes with transition metals ions favor the transfer of the metal into the gas phase by stabilizing it. Using salts of double charged ions ($M^{II}X_2$) as an example, ESI of $[M^{II}L + X_2]$ complexes may afford singly $[M^{II}L + X]^+$ or doubly $[M^{II}L]^{2+}$ charged ions by losing one or two counter-ions (X^-), respectively. In some cases, it is possible to observe ions in the ESI mass spectrum corresponding to $[M^{II}L - H]^+$, due to the elimination of one counter ion plus a subsequent expulsion of the counter anion acid (HX). The proton is therefore provided by the ligand. Meanwhile, in all these cases the oxidation state of the metal center does not change [21], the coordination number can indeed change, as Vachet and co-workers suggested. For a number of Ni^{II} and Cu^{II} complexes, the coordination numbers differ on going from solution to gas phase [22].

All these cases suggest the necessity to perform a rigorous analysis to probe unambiguously that the species detected by ESI are the ones prevailing in solution, and more importantly to confirm that they are indeed reactive intermediates on the reaction path. An important methodology is to isolate in the gas phase the species assumed to participate in the reaction mechanism and perform ion/molecule reactions with the substrate of the reaction solution [6]. This methodology is very useful to discard side-products and to assure the reliability of the analysis. Another important method is the study of well-known reactions and compares the data obtained by ESI-MS with other spectroscopic techniques.

2. Methods developed to study reaction mechanisms

There are two different possibilities for study a reaction using API methods, i.e., off-line and on-line screenings. Early investigations using API techniques were mostly performed off-line, like the oxidation of tetrahydropterins to radical cations [23], the Mitsunobu and Wittig reactions [24], and homogeneously catalyzed reactions such as the Suzuki reaction [25] or the palladium-catalyzed oxidative self-coupling of areneboronic acids [26]. The first on-line mass spectrometric investigation in electrochemical reactions using thermospray ionization was reported as early as 1986 [27]. It proved the potential-dependent formation of dimers and trimers in the electrooxidation of *N*,*N*-dimethylaniline in an aqueous solution. Another example of on-line investigations is the reaction of ferric bleomycin and iodosylbenzene, where a low dead volume-mixing tee directly attached to the spray source [28] was used.

2.1. Off-line monitoring

A sequence of events in the study of a reaction in solution by mass spectrometry could be to investigate the specific reaction conditions by mixing the reagents for the detection of the different intermediates, and then determine the solution composition over time when the reactants are progressively transformed into products. This latest operation can be accomplished by direct screening by MS of the reaction intermediates during pre-defined intervals and characterization by MS/MS, always if there is a reasonable concentration of them in solution, and these species are not degraded within few minutes. The overall time resolution has to match the rate of the process to yield the desired information. It is determined by the interval elapsed between consecutive sampling operations and is a direct function of the time used to secure and quench each aliquot in off-line methods. Transient species cannot be therefore analyzed with this feature due to their short lifetime residence in solution.

Hinderling and Chen [29] used the off-line monitoring in developing a mass spectrometric assay of polymerization catalysts for combinational screening. A homogeneous Brookhart polymerization catalyzed by a Pd(II) diimine complex using various ligands was quenched and then studied by ESI-MS. The mass spectrometric method required milligrams quantities of catalyst, took place in only few minutes, and was suitable for both pooled and parallel screens of catalyst libraries. This intriguing method of high-throughput screening of homogeneous catalyst by electrospray ionization tandem mass spectrometry was recently reviewed [30].

2.2. On-line monitoring

In the second scenario, the kinetic and mechanistic informations about the reactions in solution can be studied using reactors coupled to the ESI ion-source. This method provides mass-specific characterization of stable products and reactive intermediates with lifetimes down to the millisecond time regime.

The simplest reactor on-line coupled to the mass spectrometer is the own syringe. It allows the screening of the reaction in real time, and the trapping of transient species. Several groups developed different devices for study the mechanism in solution of radical initiated, photochemical, electrochemical and organometallic reactions, reducing the transit time of the species during the experiments. Some of them are commented below.

2.2.1. On-line microreactor [28,31,32]

A commercially available microreactor (Alltech, PEEK mixing tee, Fig. 1) can be directly connected to the ESI spray capillary, allowing to cover reaction times from 0.7 to 28 s in a continuous-flow mode. Longer reaction times can easily be covered introducing a fused silica transfer capillary of variable length between the microreactor and the spray capillary. The chemical reaction in this system takes place by mixing two liquid flows containing the substrate and the reagent in the close proximity of the ionization source. In the moment of mixing both solutions, the reaction is initiated and the mass spectra of the reacting solution under steady state conditions can be acquired.

2.2.2. On-line capillary mixer adjustable reaction chamber

The Wilson's on-line continuous-flow apparatus [33] consists in two concentric capillaries, each of which is connected

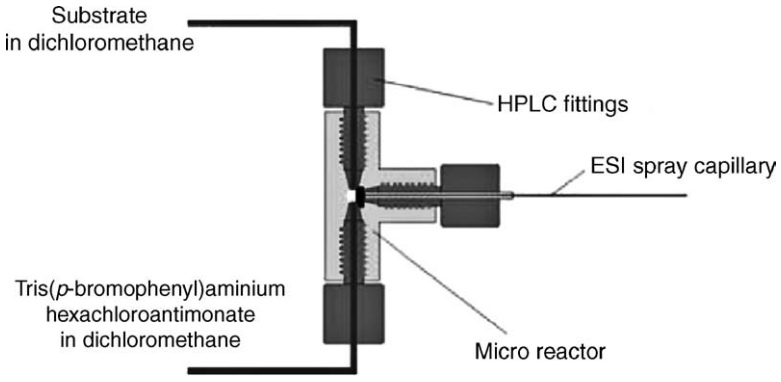

Fig. 1. The microreactor allows the effective mixing of the reactants in solution and is coupled directly to the electrospray ion source. Figure gives the set up used to study radical cation chain reactions as described in Section 3.1.

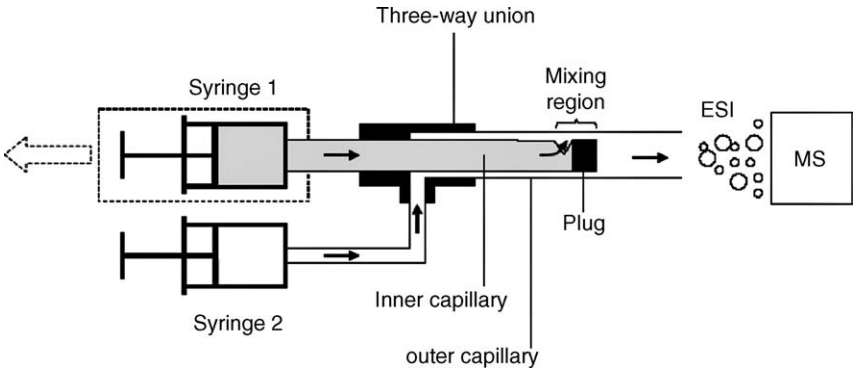

Fig. 2. Schematic representation of a continuous-flow mixing set up for kinetic measurements by time-resolved ESI-MS. Syringes 1 and 2 deliver a continuous-flow of reactants; mixing of the two solutions initiates the reaction of interest. The plug at the end of the inner capillary ensures that all the liquid from syringe 1 is expelled through a notch at the capillary end into the narrow inter-capillary space. The inner capillary can be automatically pulled back, together with syringe 1 (as indicated by the dashed arrow). This provides a means to control the "age" (reaction time) of the mixture at the capillary outlet. Arrows indicate the direction of liquid flow.

to a syringe to allow for infusion of two reactant solutions. The two solutions are mixed at the end of the inner (fused silica) capillary, and the reaction is allowed to proceed until pneumatically assisted ESI occurs at the outlet of the outer (stainless steel) capillary. The reaction time is controlled by the flow rates from the syringes, and by the volume between the mixing point and the outer capillary outlet. Mass spectra can be recorded for selected reaction times by controlling the syringes flow rate and the volume available between the capillaries ends. To acquire kinetic data (i.e., intensity time profiles), the inner capillary is withdrawn continuously such that time-dependent changes in signal intensity can be observed for all ions in the mass spectrum. A continuous-flow setup for "time-resolved" ESI-MS is depicted in Fig. 2. This system represents a concentric capillary mixer with adjustable reaction chamber volume. This instrument operates under laminar flow conditions, a fact that has to be taken into account for the data analysis. Reactant solutions are continuously expelled from two syringes. The first of these syringes is connected to the inner capillary, whereas the solution delivered by the second syringe flows through the outer capillary. The reaction of interest is initiated by mixing the two solutions at the end of the inner capillary. The reaction then proceeds, while the mixture flows towards the outlet of the apparatus, where ESI takes place. The reaction time is determined by the solution flow rate, the diameter of the outer tube and, most importantly, by the distance between the mixing point and the outlet. This distance can be modified by adjusting the position of the inner capillary, as indicated in Fig. 2. Kinetic experiments are typically performed by initially suppressing the volume between capillaries, which corresponds to a reaction time of zero. The mass spectrometer then continuously monitors the ions emitted from the capillary outlet meanwhile, the volume and the reaction time was increased by slowly pulling back the inner capillary. These experiments provide three different sets of data, i.e., the reaction time determined by the mixer position, the information on the identity of the species in the reaction mixture provided the m/z values, and the concentration of each of these species, which is related to the intensity recorded for the ions in the mass spectra. The time resolution of this system is suitable for measuring rate constants in the range from 1.0 s^{-1} up to at least 100 s^{-1}.

2.2.3. On-line quartz photolysis cell

Arakawa's on-line apparatus consists by directly irradiating a sample solution passing through a quartz photolysis cell located in the middle of the ESI spray tip to detect intermediates with lifetimes of more than few minutes (Fig. 3). A light shutter equipped with a W cutoff filter is mounted at the exit of the lamp to control photoirradiation. This set allows two different modes of irradiation. The first one, defined as cell mode irradiation, consists in the direct irradiation of the sample solution as it passing through the cell (Fig. 3). It takes about 2 min for the flowing sample to pass across the irradiated area in the cell and about 40 s to arrive at the tip of needle for spraying, which allow the mass analysis of photoproducts with lifetimes of minutes [34]. The second mode, defined as spray mode, involves the irradiation of the charged droplets distributed in a plume fashion at the tip of the needle, making possible the detection of intermediates with lifetime of milliseconds.

2.2.4. On-line photochemical reactor

Similar time resolution was described by Brum and Dell'Orco [35] monitoring the photolysis of idoxifene in a jacketed reactor. In this particular study the signal of the relevant $[M+H]^+$ ions was directly used without previous isolation, demonstrating the potential utility of such MS interfaces for in situ probing.

The experimental approach consists in a jacketed reaction flask equipped with a looping stainless steel capillary (Fig. 4), where the solution is irradiated. A pump allows the circulation of the solution trough the capillary at a high flow rate (5–10 mL min^{-1}), meanwhile, another separates part of the circulating solution into a PEEK tubing. Finally, a third pump allows a posterior addition of buffer solution or make-up solvent appropriate for the ionization method through a static mixing tee. The accuracy of the fluid flow is ensured by the use of a metering valve in the connection between the looping capillary and the PEEK tubing. This apparatus allows the introduction of samples to the mass spectrometer with an approximate dead time of few minutes, making it not suitable for extremely rapid reactions. However, it can be used to study a very great variety of not only photochemical, but also organic reactions in real time period [36] and in a processing scale of the reactants.

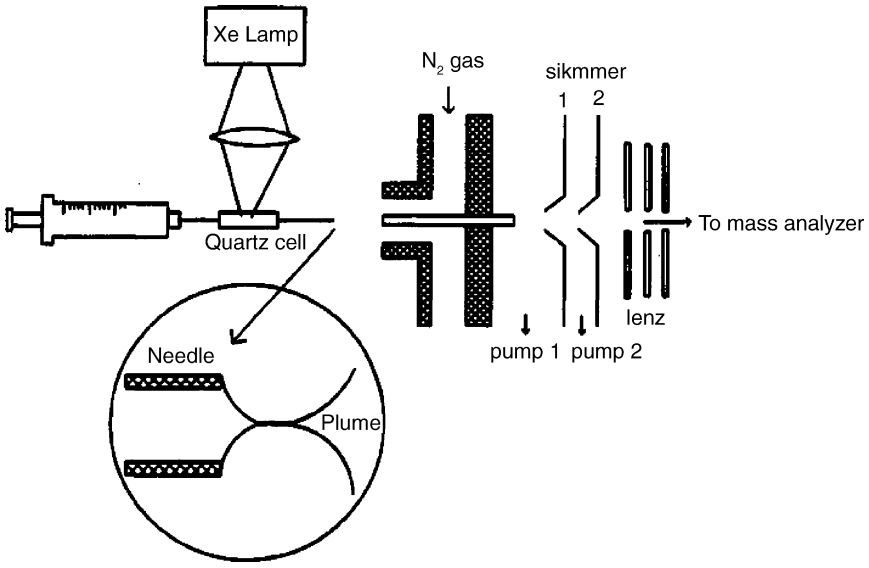

Fig. 3. Schematics of electrospray mass spectrometry for on-line analysis of photochemical reactions. Two modes of photoirradiation ($\lambda > 420$ nm; a UV cutoff filter) were used: the cell mode, involving irradiation of the sample solution in a quartz cell, and the spray mode, involving irradiation of charged droplets distributed in the plume at the tip of needle [34].

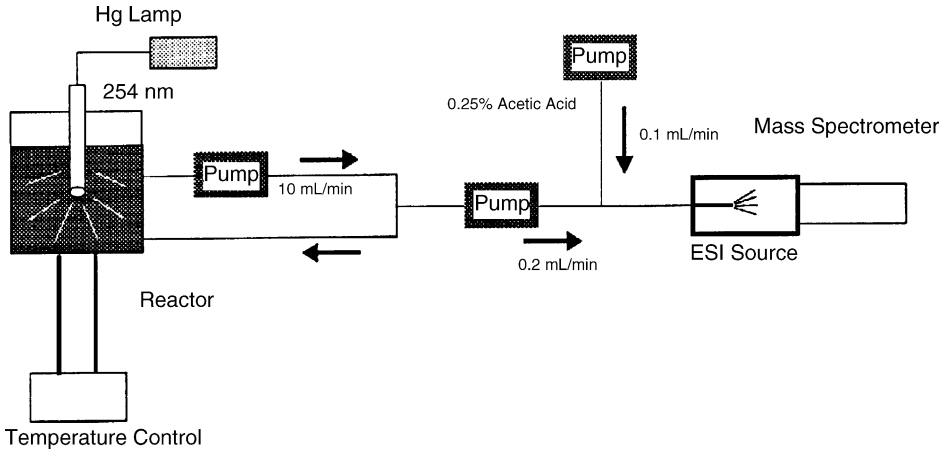

Fig. 4. Basic scheme of the experimental apparatus [35].

2.2.5. On-line photochemical apparatus

Amster's apparatus is an on-line ESI-MS technique for the study of photochemical reactions that greatly reduces the transit time of photogenerated species [37]. Fig. 5 shows sample solutions that are irradiated directly in the optically transparent nanospray tip of the ESI source. Subsequent thermal reactions of the primary photoproducts take place in the region between the photolysis zone and the tip end. The transit time of a photoproduct depends on the volumetric flow rate of the sample, the inner diameter of the tip, and D, the distance between the midpoint of the irradiated zone and the tip end. For example, with $D = 0.84$ mm, a tip diameter of 40 μm, and a flow rate of 40 μL h^{-1}, products require 95 ms to arrive at the tip end for spraying. All chemical reactions are quickly quenched (μs time scale) once the sample solution leaves the tip owing to rapid desolvation of the solutes that occurs during the electrospraying process. Consequently, ionic species with solution lifetimes in the millisecond range or longer can be detected by this technique.

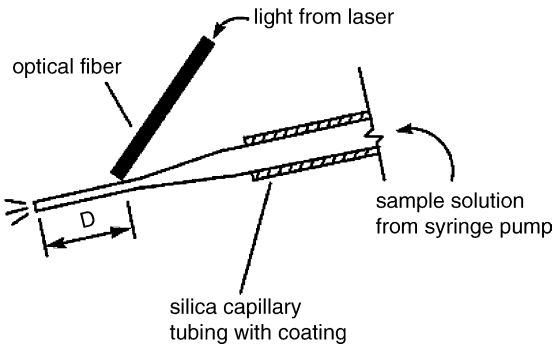

Fig. 5. Photochemical apparatus for nanospray tip [37].

2.2.6. On-line electrochemical cell

Lev and co-workers [38] developed a radial flow electrochemical cell coupled to an electrospray interface to study

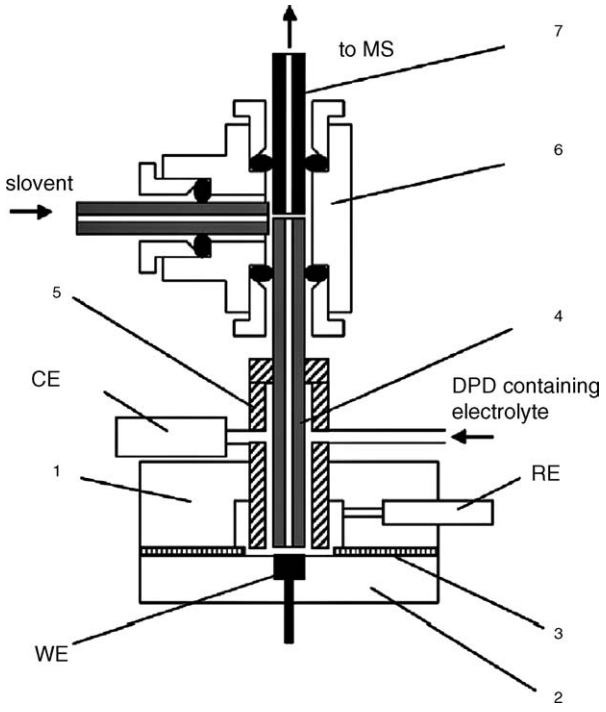

Fig. 6. Scheme of the Lev's radial thin layer flow cell. (1) Upper Delrin block with tubings; (2) bottom Delrin block with Pt working disk electrode; (3) Teflon spacer; (4) reactor-PEEK tube o.d. 1.57 mm; (5) PEEK tube o.d. 3.2 mm, i.d. 1.6 mm; (6) T-junction; (7) grounded stainless steel tube approx. 5 cm long, i.d. 0.13 mm, o.d. 1.6 mm [38].

electrochemical reactions involving subsequent parallel and consecutive chemical reactions (Fig. 6). The electrochemical flow cell consists of two cylindrical Delrin blocks (1 and 2) separated by a 50 μm Teflon spacer (3). A 1.6 mm diameter Pt disk electrode (WE) is pressed into the lower block. The electrolyte flows in a radial, inward direction. A central aperture in the Teflon spacer (3) allows passage of the electrolyte towards the center of the disk electrode where it is collected into the axial inner tube (4). The volume of the compartment of the working electrode, which is the volume of electrolyte located between the working electrode and the walls of the central tube (4), is only 0.1 μL. The working disk electrode and the inner tube (4) are coaxial. The channel in the central tube (4) forms a reactor in which subsequent chemical reactions can occur, and its volume can be adjusted to 0.5, 2.0, 2.8, and 8.0 μL through different inner PEEK tubes, covering reaction times from 4.3 to 480 s. A detailed description of on-line coupling of electrochemical apparatus to mass spectrometers can be found in the review by Diehl and Karst [9].

3. Radical reactions

Some synthetically important radical reactions have been studied by API-MS methods. The transient radicals were unambiguously detected and characterized by MS/MS methods.

3.1. Radical cation chain reactions

3.1.1. [2 + 2]-Cycloaddition of trans-anethole

Meyer and Metzger [32,39] studied the *tris*(*p*-bromophenyl)aminium hexachloroantimonate ($\mathbf{1}^{\bullet+}SbCl_6^-$) mediated [2 + 2]-cycloaddition of *trans*-anethole (**2**) to give 1,2-*bis*-(4-methoxyphenyl)-3,4-dimethyl cyclobutane (**3**). The reaction proceeds as a radical cation chain reaction via transients $\mathbf{2}^{\bullet+}$ and $\mathbf{3}^{\bullet+}$ that were unambiguously detected and characterized by ESI-MS/MS directly in the reacting solution. At first, the reaction was studied by APCI-MS, because substrate **2** and product **3** are not ionized by ESI. A solution of $\mathbf{1}^{\bullet+}SbCl_6^-$ and a solution of **2**, both in dichloromethane, were mixed in a microreactor system (Scheme 1), feeding continuously the APCI-MS. Thus, the reaction could be followed by APCI making sure that a solution containing an ongoing radical cation chain reaction was introduced in the ion source. This is of central importance because an ongoing reaction process is necessary for a successful detection by ESI-MS of intermediates under steady state conditions.

When the reacting solution of $\mathbf{1}^{\bullet+}SbCl_6^-$ and **2** was examined by ESI-MS, the spectrum depicted in Fig. 7(a) was collected. The ESI-MS spectrum only displays an intensive signal of radical cation $\mathbf{1}^{\bullet+}$. Substrate **2** and product **3** are not ionized during the ESI process and cannot be observed. The transient radical cations $\mathbf{2}^{\bullet+}$ of *m*/*z* 148 and $\mathbf{3}^{\bullet+}$ of *m*/*z* 296 were not recognized in the spectrum directly, since the quasi stationary concentration of the intermediates in the radical cation chain reaction is estimated to be approximately 10^{-7} M, three orders of magnitude lower than the concentration of radical cation $\mathbf{1}^{\bullet+}$. The signals of the transient radical cations are expected to disappear in the chemical noise. Zooming into the chemical noise, it is possible to recognize the very weak signals at the expected *m*/*z* of the radical cations. Using the MS/MS technique radical cation $\mathbf{2}^{\bullet+}$ (Fig. 7(b)) and $\mathbf{3}^{\bullet+}$ (Fig. 7(c)) were clearly detected. The ESI-MS/MS spectra were in agree with those of the respective authentic radical cations characterized by APCI-MS/MS.

3.1.2. Electron transfer initiated Diels–Alder reactions

Using a microreactor coupled API-MS (Fig. 1), Fürmeier and Metzger investigated the *tris*(p-bromophenyl)aminium hexachloroantimonate ($\mathbf{4}^{\bullet+}SbCl_6^-$, 5.0 mmol L^{-1}) initiated reaction of phenylvinylsulfide (**5**, 0.5 mmol L^{-1}) and cyclopentadiene (**6**, 2.5 mmol L^{-1}) in dichloromethane, which gives the respective Diels–Alder product **7** [40]. This preparatively interesting reaction proceeds as radical cation chain reaction via the transient radical cations $\mathbf{5}^{\bullet+}$ of the dienophile and $\mathbf{7}^{\bullet+}$ of the respective Diels–Alder addition product (Scheme 2). These radical cations could be detected directly and characterized unambiguously in the reacting solution by ESI-MS/MS. Their identity was confirmed by comparison with MS/MS spectra of authentic radical cations $\mathbf{5}^{\bullet+}$ and $\mathbf{7}^{\bullet+}$obtained by APCI-MS, and by CID experiments of the corresponding molecular ions generated by EI-MS. In addition, substrates and products could be monitored easily in the reacting solution by APCI-MS.

Furthermore, Fürmeier and Metzger used the same procedure to study the electron transfer initiated Diels–Alder reaction of

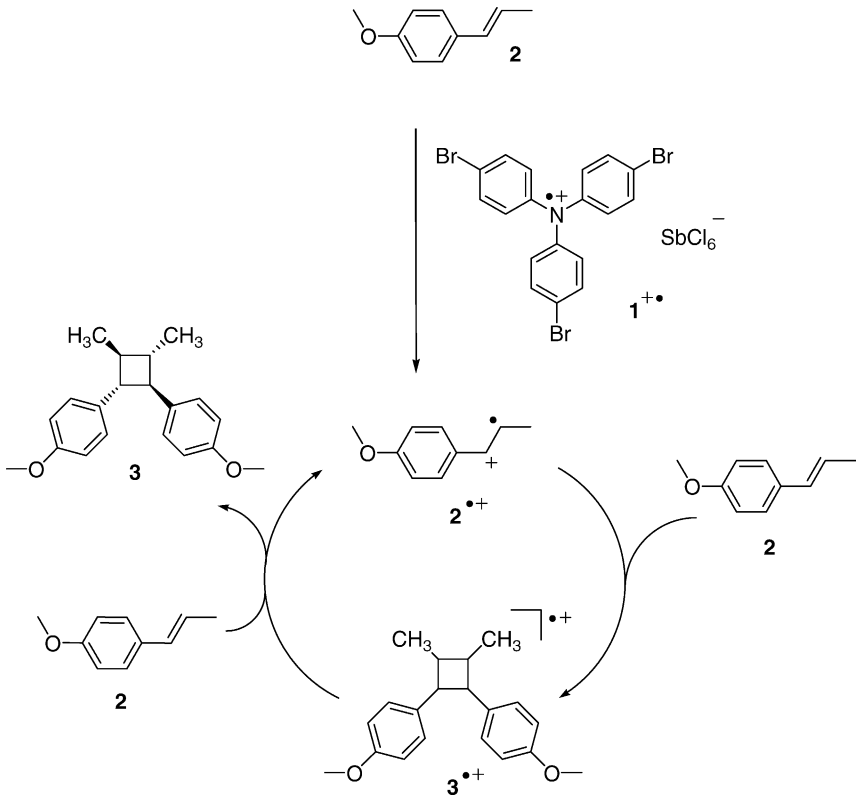

Scheme 1. *Tris*(*p*-bromophenyl)aminium hexachloroantimonate ($I^{\bullet+}SbCl_6^-$) mediated radical cation chain reaction of *trans*-anethole (**2**) to give head-to-head *trans*,*anti*,*trans*-1,2-*bis*-(4-methoxyphenyl)-3,4-dimethyl cyclobutane (**3**) via the reactive intermediates $\mathbf{2}^{\bullet+}$ and $\mathbf{3}^{\bullet+}$ [32,39].

isoprene and anethole, as well as the Diels–Alder dimerization of 1,3-cyclohexadiene. They unambiguously detected and characterized the respective transient radical cations of the dienophiles and of the Diels–Alder addition products [40].

3.2. Radical chain reactions

Free radicals are neutral species and therefore cannot be normally detected by ESI-MS. However, it is well known that radical reactions can be mediated by Lewis acids if the substrate acts as a Lewis base by chelating the metal atom of a Lewis acid in solution. Fürmeier and co-workers studied tin hydride mediated radical additions to dialkyl 2-alkyl-4-methyleneglutarates in the presence of Lewis acids (Scheme 3) [31,41]. Diesters such as dialkyl glutarates were able to chelate the Lewis acid and form the dialkyl glutarate–Lewis acid complex, thus allowing the detection of the Lewis acid–ester complexes by ESI-MS. For example, the complex with $Sc(OTf)_3$ dissociates to form a chelate complex cation and a triflate anion was intercepted. In addition to monomeric also dimeric complex ions $[\mathbf{8}_2{\cdot}Sc_2(OTf)_5]^+$ were observed, giving evidence of the respective dimeric complexes in solution [42].

The reaction was carried out by mixing a solution of glutarate **9** with **8** and $Sc(OTf)_3$ in diethyl ether, saturated with air and a solution of tributyltin hydride containing triethylborane under argon in the microreactor on-line coupled to the ESI ion source (Fig. 1). The reacting solution was fed continuously into the mass spectrometer. In Fig. 8(a), the mass spectrum of the reacting solution after a reaction time of approximately 30 s is depicted. Monomeric and dimeric complex ions of substrate **9** and product **10** can be observed.

Furthermore, heterodimeric complex ions of substrate and product $[\mathbf{9}{\cdot}\mathbf{10}{\cdot}Sc(OTf)_2]^+$ and $[\mathbf{9}{\cdot}\mathbf{10}{\cdot}Sc_2(OTf)_5]^+$, respectively, were observed. An intermediate radical complex ion $[\mathbf{11}{\cdot}Sc(OTf)_2]^+$ with an expected *m*/*z* ratio of 654 could not be unambiguously detected in the mass spectrum (Fig. 8(a)) due to the steady state concentration of radical **11** in the radical chain reaction, which is estimated to be approximately 10^{-7} M, four orders of magnitude lower than the concentration of substrate **9** and of product **10**.

Using MS/MS it was also possible to detect and characterize the intermediate radical **11** as a monomeric complex ion $[\mathbf{11}{\cdot}Sc(OTf)_2]^+$ (*m*/*z* 654, Fig. 8(b)) as well as a heterodimeric complex ion with substrate **9** and product **10**, respectively. The MS/MS spectrum of the heterodimeric complex ion of substrate and radical $[\mathbf{9}{\cdot}\mathbf{11}{\cdot}Sc_2(OTf)_5]^+$ (*m*/*z* 1400) is depicted in Fig. 8(c).

Two main and characteristic fragmentations of this ion are the dissociation by the loss of neutral radical complex $\mathbf{11}{\cdot}Sc(OTf)_3$ (−803 u) that gives the substrate complex ion $[\mathbf{9}{\cdot}Sc(OTf)_2]^+$ (*m*/*z* 597), and the loss of neutral substrate complex $\mathbf{9}{\cdot}Sc(OTf)_3$ (−746 u) results in the radical complex ion $[\mathbf{11}{\cdot}Sc(OTf)_2]^+$ (*m*/*z* 654). Additionally, a fragmentation to complex ion $[\mathbf{9}{\cdot}\mathbf{11}{\cdot}Sc(OTf)_2]^+$ (*m*/*z* 908) by loss of $Sc(OTf)_3$ (−492 u) was observed. The elemental composition of the ions $[\mathbf{11}{\cdot}Sc(OTf)_2]^+$, $[\mathbf{9}{\cdot}\mathbf{11}{\cdot}Sc_2(OTf)_5]^+$, and $[\mathbf{10}{\cdot}\mathbf{11}{\cdot}Sc_2(OTf)_5]^+$

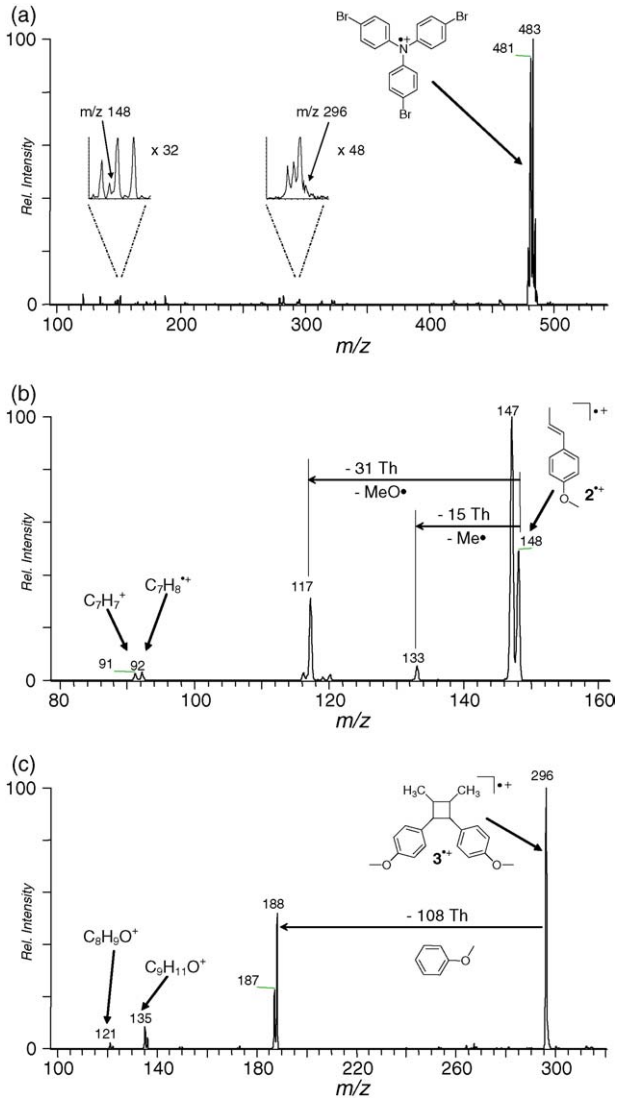

Fig. 7. (a) ESI mass spectrum in the positive ion mode of the reacting solution of *trans*-anethole (**2**) (0.5 mmol L^{-1}) and *tris*(*p*-bromophenyl)aminium hexachloroantimonate (**1**) (5.0 mmol L^{-1}) in dichloromethane (reaction time approx. 7 s). (b) ESI-MS/MS of the ion of *m/z* 148 of the same reacting solution showing identical fragmentations compared to the APCI-MS/MS spectrum of the authentic radical cation $\mathbf{2}^{\bullet+}$ c) ESI-MS/MS of the ion of *m/z* 296 of the same reacting solution showing identical fragmentations compared to the APCI-MS/MS spectrum of the authentic radical cation $\mathbf{3}^{\bullet+}$.

were confirmed via their accurate masses determined by Q-TOF measurements.

The radical chain allylation of diethyl 2-iododiadipate with allyltributyltin in the presence of $Sc(OTf)_3$ to give diethyl 2-allyladipate via a radical intermediate was studied quite analogously. The transient diester radical was detected and characterized by MS/MS [31].

3.3. Various radical reactions

Hess et al. [43] reported the degradation products resulting from modified Fenton reactions with the nitroaromatic compounds trinitrotoluene (TNT) and trinitrobenzene (TNB) through electrospray ionization tandem mass spectrometry (off-line ESI-MS^n). Several hydroperoxide adducts were tentatively identified as initial, one-electron reduction products of TNT, and their structure confirmed by tandem mass spectrometry.

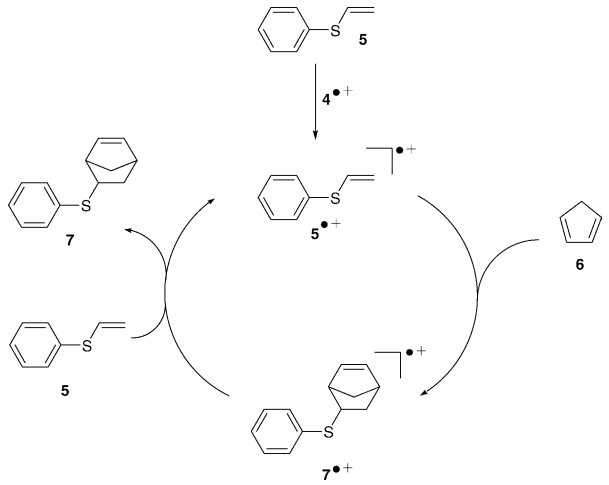

Scheme 2. *Tris*(*p*-bromophenyl)aminium hexachloroantimonate ($\mathbf{4}^{\bullet+}SbCl_6^-$) initiated radical cation chain reaction of phenylvinylsulfide (**5**) and cyclopentadiene (**6**) to give the Diels–Alder product 5-(phenylthio)norbornene (**7**) via the reactive intermediates $\mathbf{5}^{\bullet+}$ and $\mathbf{7}^{\bullet+}$.

Griep-Raming and Metzger [44] studied the thermal dissociation of the triphenylmethyl dimer and of *tetra*(*p*-anisyl) hydrazine, operating the ESI source as electrolytic cell to ionize neutral species, e.g., the triphenylmethyl radical. In this study, an electrospray ionization source able to heat the spray capillary was used.

3.4. Photochemical reactions

Arakawa et al. [45] developed the on-line photoreaction cell depicted in Fig. 3, and performed a series of studies on the detection of reaction intermediates in photosubstitution and photooxidation of Ru(II) complexes. The photosubstitution of $Ru(bpy)_2B^{2+}$ [bpy = 2,2′-bipyridine; B = 3,3′-dimethyl-2,2′-bipyridine (dmbpy) or 2-(aminomethyl)pyridine (ampy)] was studied in acetonitrile and pyridine. Irradiation of

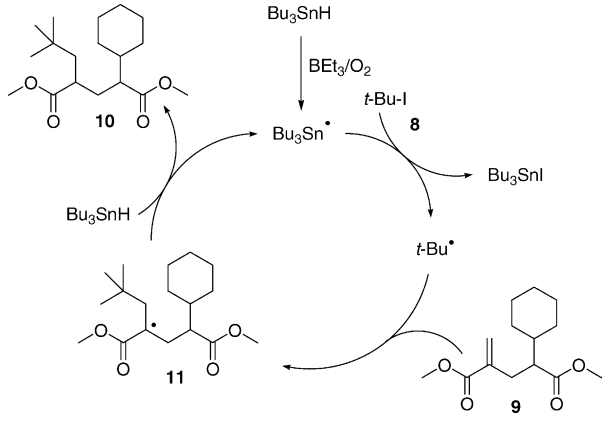

Scheme 3. Tributyltin hydride-mediated addition of *tert*-butyl iodide (**8**) to dimethyl 2-cyclohexyl-4-methyleneglutarate (**9**), stereoselectively giving *syn*-dimethyl 2-cyclohexyl-4-neopentyl-glutarate (**10**) via transient adduct radical **11** in the presence of $Sc(OTf)_3$.

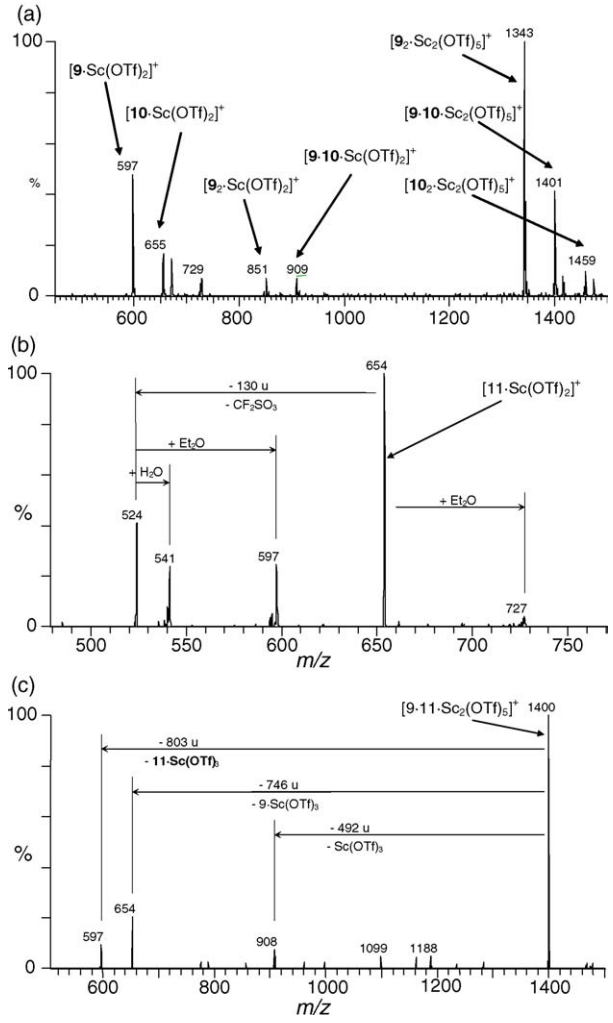

Fig. 8. (a) ESI mass spectrum in the positive ion mode of the reacting solution of the tributyltin hydride-mediated addition (1.25 mmol L^{-1}) of *tert*-butyl iodide (**8**) (2.0 mmol L^{-1}) to dimethyl 2-cyclohexyl-4-methyleneglutarate (**9**) (0.5 mmol L^{-1}) in the presence of scandium triflate (0.6 mmol L^{-1}) in diethyl ether resulting in addition product **10** after a reaction time of approximately 30 s. (b) ESI-MS/MS of the radical complex ion $[\mathbf{11}\cdot Sc(OTf)_2]^+$ (*m*/*z* 654). (c) ESI-MS/MS of the substrate–radical complex ion $[\mathbf{9}\cdot\mathbf{11}\cdot Sc_2(OTf)_5]^+$ of *m*/*z* 1400 from the same reacting solution.

$Ru(bpy)_2B^{2+}$ and related complexes yields a charge-transfer excited species with an oxidized Ru center and an electron localization on the bpy moiety. The excited-state complex underwent ligand substitution via a stepwise mechanism that includes a η^1 bidentate ligand (Scheme 4). Photoproducts such as $Ru(bpy)_2S_2^{2+}$ (S = solvent molecule) and intermediates with a monodentate (mono-*hapto*-coordination) B ligand, $Ru(bpy)_2BS^{2+}$, and $Ru(bpy)_2BSX^+$ ($X = C1O_4^-$, PF_6^-) were detected. Other studies also identified photooxidized products of several mixed–valence Ru(II) complexes upon irradiation ($\lambda > 420$ nm) [34b,46].

A novel photochemical switching reaction utilizing ESI-MS was reported by Arakawa and co-workers [47] (Scheme 5). This process involved a cation (e.g., K^+, Na^+) binding complex that consisted of a malachite green derivative incorporating a *bis*(monoazacrown ether), **12**. The irradiation (240–400 nm) of a solution of crowned malachite green containing an equimolar amount of potassium or sodium perchlorate resulted in an ESI-MS signal which was assigned to the corresponding quinoid cation and subsequent loss of the metal ion, **13**. Presumably, the metal ion was released upon charge–charge repulsion, followed by the intramolecular ionization of the leuconitrile moiety (Scheme 5). The 'off' or 'on' mode of a cation binding host could be manipulated by UV irradiation and confirmed by ESI-MS analysis.

The same on-line photochemical ESI-MS methodology was employed in the analysis of photoallylation reactions of dicyanobenzene (DCB) by allylic silanes via photoinduced electron transfer [48]. Brum and Dell'Orco [35] reported on investigations of the photolysis of a substituted triphenylethylene derivative using the reactor depicted in Fig. 4. The approach allowed the monitoring of the parent species and five relevant reaction products simultaneously. The rate constants for photoconversion could be derived from the time-ion current data. Herein, Schuster et al. used ESI-MS to study off-line some photoadditions to C_{60} [49].

Amster and co-workers [37] reported the use of ESI-MS to probe the solution photochemical behavior of $[CpFebz]PF_6$, where Cp is η^5-cyclopentadienyl and bz is η^6-benzene, applying the apparatus proposed by the group shown in Fig. 5. The interest in the $[CpFe(\eta^6\text{-arene})]^+$ family arises from their use as visible-light-sensitive photoinitiators for the

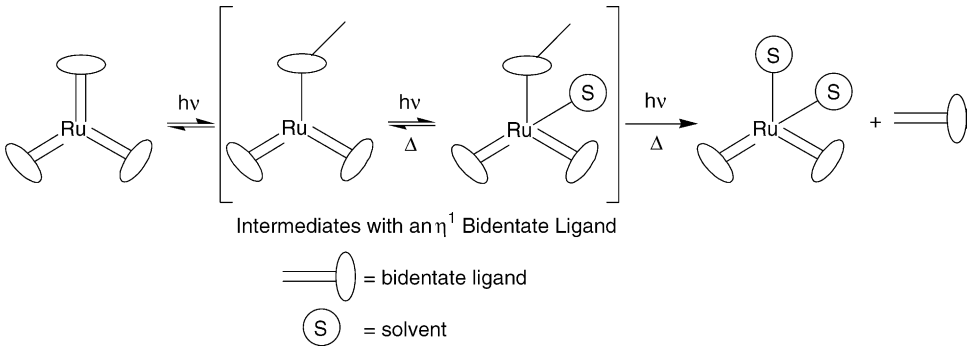

Scheme 4. Photooxidation of ruthenium complexes.

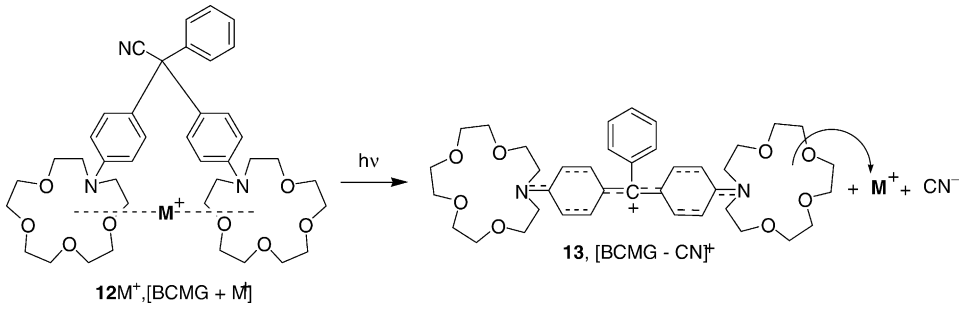

Scheme 5. Photochemical switching reaction with Na^+ and K^+ as an 'off' or 'on' mode of a cation binding host. The screening was performed with substrate concentrations around 0.2 mmol L^{-1} in acetonitrile as solvent.

polymerization of epoxides and other monomers. Mechanistic studies by several groups have established key features of the solution photochemistry of these mixed–ring sandwich complexes [50]. The proposed mechanism corroborated by Amster proceeds by ligand field photoexcitation inducing loss of arene to produce $[CpFe(L)_3]^+$. The irradiation of an acetonitrile solution of $[CpFebz]^+$ in the nanospray tip of the ESI source yields two major series of ionic products: $[CpFe(MeCN)_{2–3}]^+$ and $[Fe(MeCN)_{3–6}]^{2+}$. The first series results from the photoinduced release of benzene from the parent complex (Eq. (1)), while the second series reflects the subsequent thermal disproportionation of the half-sandwich product (Scheme 6). From the experimental data, a lifetime of 95 ms for $[CpFe(MeCN)_3]^+$ in room temperature acetonitrile was derived. Irradiating $[CpFebz]^+$ in an MeCN solution containing up to 400 mM cyclohexene oxide (CHO) yielded the same products observed in the pure solvent. In addition, species

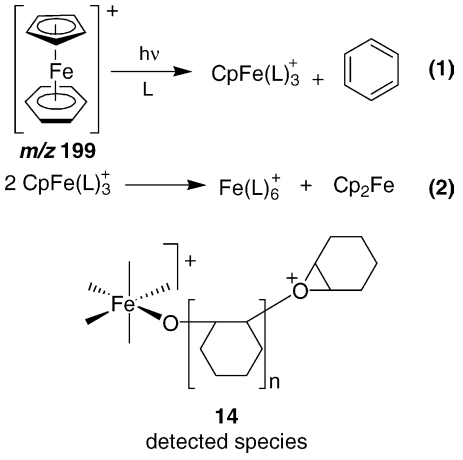

Scheme 6. Iron-containing product **14** detected in photolyzed solutions of $[CpFebz]^+$ (0.041 mmol L^{-1}) and cyclohexene oxide (CHO, 40 mmol L^{-1}) in 1,2-dichloroethane employing the microreactor depicted in Fig. 5.

containing coordinated CHO, such as $[Fe(MeCN)_3(CHO)]^{2+}$ and $[Fe(MeCN)_4(CHO)]^{2+}$, become increasingly abundant at the higher epoxide concentrations. However, no products containing more than one epoxide molecule are observed, even at the highest CHO concentrations used in the experiments. This result indicates that CHO cannot compete effectively with acetonitrile for coordination sites on the metal center. Photolyzing $[CpFebz]^+$ and CHO in the poorly coordinating solvent, 1,2-dichloroethane, resulted in a much richer assortment of products. They detected half-sandwich complexes of general formula $[CpFe(H_2O)(CHO)_{0–5}]^+$, as well as fully ring-deligated complexes of general formula $[(H_2O)Fe(CHO)_{2–12}]^{2+}$ (with transit time of 50 ms). A chemically reasonable description of the structures of ions such as $[(H_2O)Fe(CHO)_{10}]^{2+}$, $[Fe(CHO)_8]^{2+}$, and $[CpFe(CHO)_5]^+$ involving a growing polymer chain bound directly to the metal center (detected as **14**, Scheme 6) was suggested. However, no further studies have been made to confirm this suggestion.Stillman and co-workers [51] reported the direct measurements of the products following the photooxidation and photoreduction of a metallophthalocyanine π-ring. ESI-MS was used to detect the anion zinc(II) (1,4,8,11,15,18,22,25-octafluoro, 2,3,9,10,16,17,23,24-octaperfluoroisopropylphthalocyaninechloride, $[ZnperF_{64}Pc(-2)(Cl)]^-$ and its π ring anion radical species, $[ZnperF_{64}Pc(-3)(Cl)]^{2-}$. The anion radical species was then photooxidized as a sacrificial photoinduced oxidizing agent using CBr_4 to produce $[ZnperF_{64}Pc(-2)(Cl)]^{2-}$. The complete reaction cycle was detected directly by ESI-MS, and reaction times of some minutes are provided (Scheme 7).

4. Electrochemical reactions [9]

Lev and co-workers studied the electrochemical oxidation of *N*,*N*′-dimethyl-*p*-phenylenediamine (DPD) in aqueous electrolyte using the reactor depicted in Fig. 6 [38]. The competitive paths of the reaction mechanism include the parallel coupling

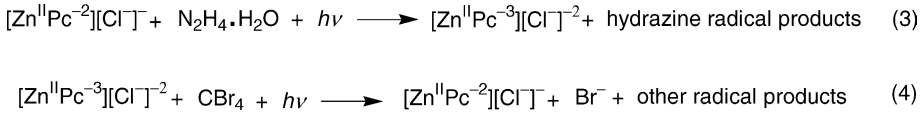

Scheme 7. Proposed mechanism of photoreduction (Eq. (3)), and photooxidation (Eq. (4)) of zinc phthalocyanine.

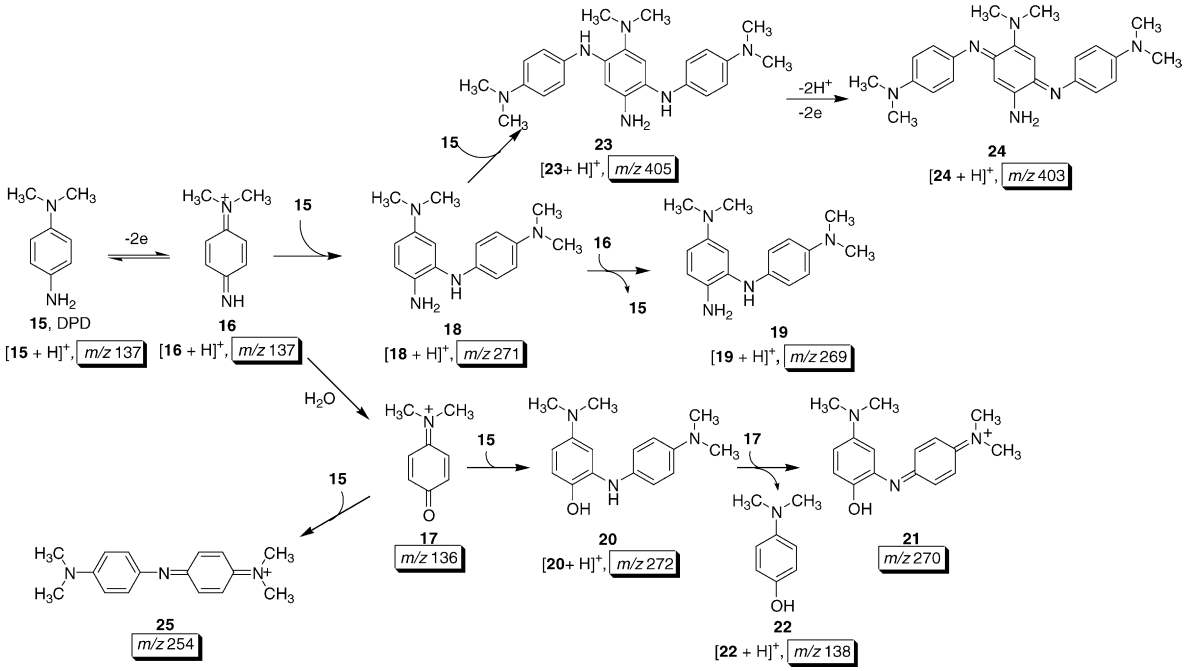

Scheme 8. Lev's on-line electrochemical-MS studies of the mechanism of oxidation of *N,N′*-dimethyl-*p*-phenylenediamine (DPD, 5.0 mmol L^{-}1) in aqueous electrolytes (0.1 mol L^{-}1).

reactions of unreacted DPD with quinonediimine, the first path, and quinonemonoimine, the second path. The latter is formed by hydrolysis of quinonediimine. The basic transformations of DPD (compound **15**) are depicted in Scheme 8. The authors mentioned that products were detected after passing through the reactor, where just chemical processes occurred, due to the relative multistage chemical coupling reactions. If the chemical reactions did not undergo in the flow cell, two electrons could be removed from each DPD molecule entering the cell, which would result in a complete transformation of DPD into quinonediimine.

5. Organocatalyzed reactions

5.1. The Baylis–Hillman reaction

Using electrospray ionization mass spectrometry in both the positive and negative ion mode, Eberlin and co-workers [52] monitored on-line the Baylis–Hillman reaction performing the reaction in the own syringe as the reactional medium (Scheme 9). The proposed intermediates for the catalytic cycle of the Baylis–Hillman reaction (**26**–**32**, Scheme 10) were successfully intercepted and structurally characterized for the first time using electrospray ionization with mass and tandem mass spectrometry. They also collected strong evidence for the currently accepted mechanism [53].

5.2. Ring contraction reaction

Looking for experimental support to validate the mechanism of ring contraction for the reaction in Scheme 11, Eberlin and co-workers [54] monitored the reaction by ESI-MS and ESI-MS/MS using the own syringe as the reactional medium. A bicyclic iminium ion intermediate $\mathbf{35}^{+}$ was proposed to participate in the reaction (Scheme 12), but both reactant **33** and product **34** were neutral molecules. These neutral species were, however, expected to be in equilibrium in solutions of protic solvents such as methanol with their protonated forms. Therefore, ESI could transfer both reactants and products to the gas phase as $[M + H]^{+}$ species for MS analysis. Even an unfavored equilibrium was helpful considering the exceptionally high sensitivity of the ESI-MS technique. First was performed the ESI-MS monitoring of the reaction of iodo-β-enamino-esters **33a–c** with Et_3N as the base. Iodo-β-enamino-esters **33** (1.0 equiv.) and Et_3N (1.0 equiv.) were mixed in 1:1 toluene/methanol (2 mL) at 25 °C, and the reaction was monitored by ESI-MS. Note

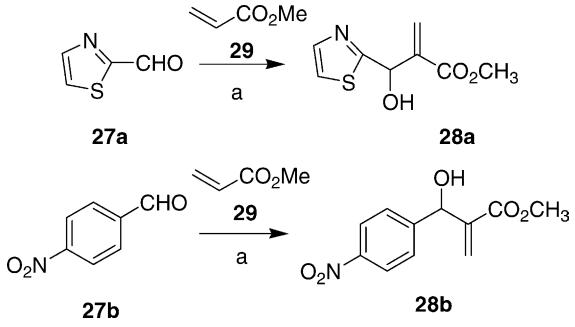

Scheme 9. Baylis–Hillman reactions monitored by ESI(+)-MS/MS. Reagents and conditions: (a) aldehyde (**27a**,**b**) (0.027 mmol L^{-1}), DABCO (**26**) (0.018 mmol L^{-1}), and methyl acrylate (**29**) (0.035 mmol L^{-1}) in MeOH at room temperature.

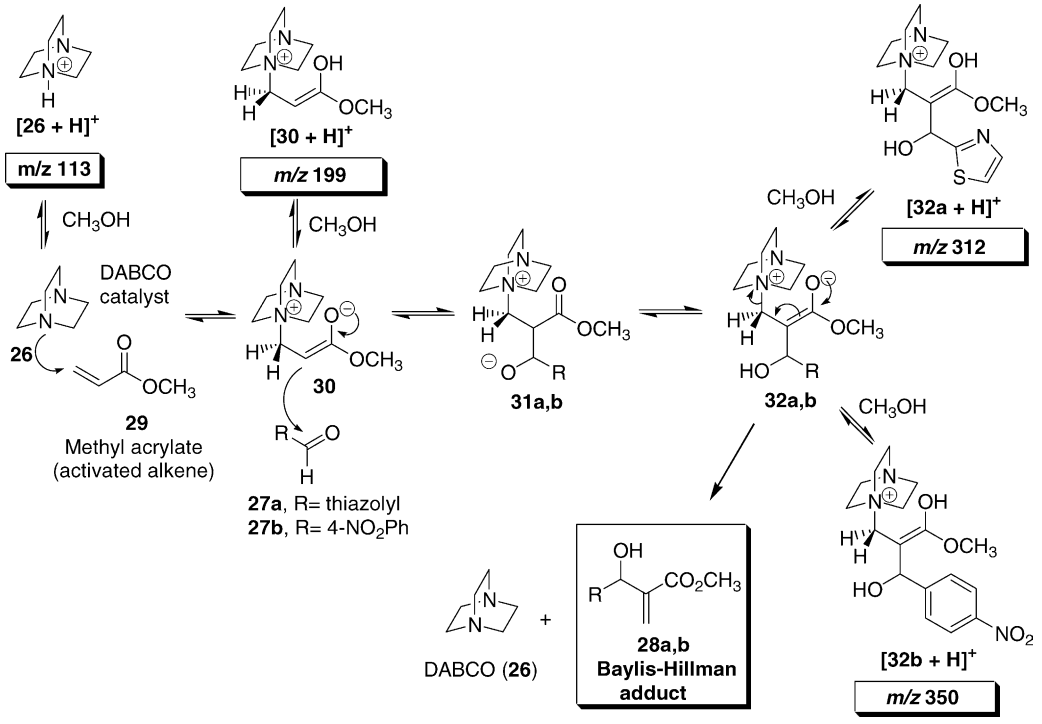

Scheme 10. Mechanism of Baylis–Hillman reaction of methyl acrylate and aldehydes catalyzed by DABCO. The protonated species expected to be intercepted and structurally characterized by ESI(+)-MS/MS, with their respective *m*/*z* ratios (flow rate of analysis 0.01 mL min^{-1}).

that even when anhydrous HPLC-grade solvents were used, traces of water needed for the last hydrolysis step that yields **34**, were likely present. Major ions were clearly detected by ESI-MS, corresponding to **33a**, the protonated reactant $[\mathbf{33a}+H]^+$ of *m*/*z* 386, intermediate $\mathbf{35a}^+$ of *m*/*z* 258, and the protonated product $[\mathbf{34a}+H]^+$ of *m*/*z* 276. Likewise for **33b** and **33c**, the protonated reactant $[\mathbf{33b}+H]^+$ of *m*/*z* 400 and $[\mathbf{33c}+H]^+$ of *m*/*z* 416, the intermediates $\mathbf{35b}^+$ of *m*/*z* 272, and $\mathbf{35c}^+$ of *m*/*z* 306, and the final protonated products $[\mathbf{34b}+H]^+$ of *m*/*z* 290 and $[\mathbf{34c}+H]^+$ of *m*/*z* 306 were clearly detected. The detected cations, as shown by continuous ESI-MS monitoring, were the same from 1 to 60 min of reaction. Scheme 12 summarizes a general reaction pathway showing neutral and protonated reactants and protonated products, as well as the key bicyclic iminium ion intermediates $\mathbf{35a–c}^+$ (with their respective *m*/*z* ratios) that have been intercepted and structurally characterized by ESI-MS(/MS).

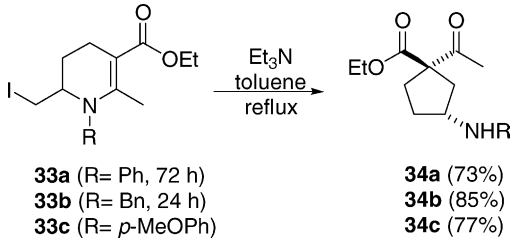

Scheme 11. Ring contraction reaction.

6. Homogeneously transition metal catalyzed reactions

6.1. Alkynilation of tellurides mediated by Pd(II)

Under palladium dichloride catalysis, vinylic tellurides couple efficiently with alkynes with retention of the double-bond geometry. Looking for experimental support to validate the catalytic cycle proposed for this reaction, Eberlin and co-workers [55] decided to investigate the coupling reaction of vinylic tellurides with alkynes promoted by $PdCl_2$ by means of mass spectrometry techniques. It was applied ESI to "fish" Pd- and Te-containing cationic intermediates involved in the reaction described in Scheme 13 directly from the reaction medium to the gas phase for ESI-MS and ESI-MS/MS analysis. Reaction of telluride **36** with alkyne **37** was performed according to Scheme 13 to give **38**. The reaction mixture was electrosprayed via the ESI source operated in the positive ion mode [56]. The reactional mixture was stirred for 1 h, the mixture gave a number of ions that were attributed to the species shown in Scheme 14. The isotopic pattern of all ions matched the calculated ones for the suggested species, in particular for those containing the multi-isotope elements tellurium and palladium.

The most relevant data for the validation of the proposed catalytic cycle was the detection of three Te and Pd-containing cationic complexes; **39** of *m*/*z* 717, **40** of *m*/*z* 499, and **41** of *m*/*z* 627. Ions **39** and **40** were suggested to be formed by solution ionization of the neutral species $LnPdCl_2$: that is, $LnPdCl_2 \rightarrow LnPdCl^+ + Cl^-$. Cations analogous to **39** and **40** have been suggested [25,57] using NMR and cyclic voltamme-

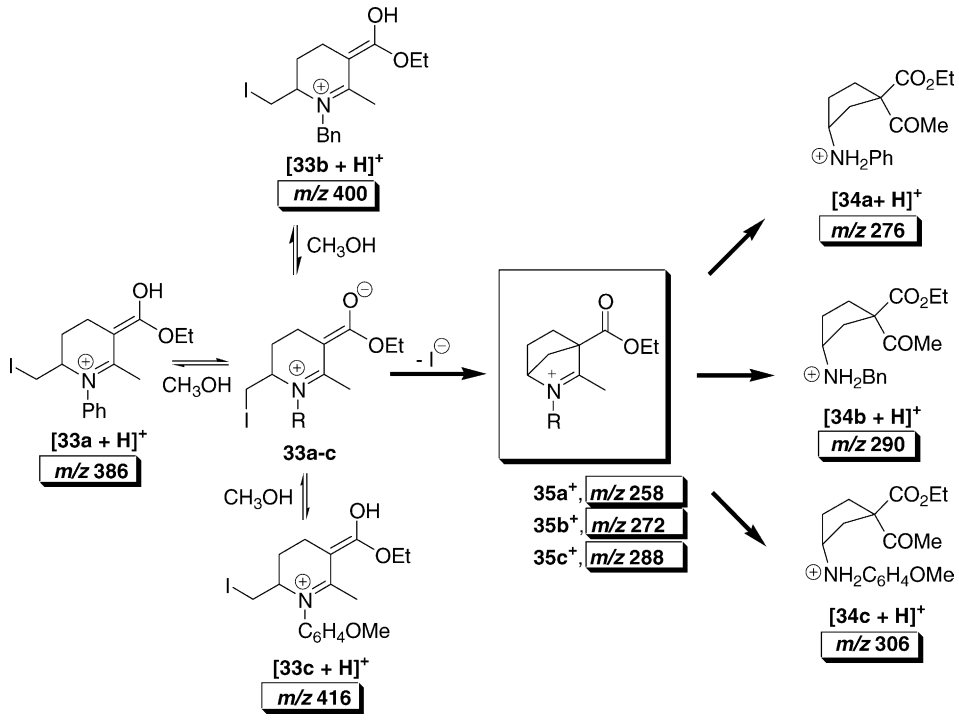

Scheme 12. Mechanism probed by ESI-MS for ring contraction reaction of iodo-β-enamino-esters. The screening was performed using **33a–c** (1 mmol), Et_3N (1 mmol) in toluene/methanol (1:1, 20 mL) at a flow rate of 0.0l mL min^{-1}.

try in reactions where $ArPd^+$ complexes were postulated. The cationic intermediates were characterized by ESI(+)-MS/MS experiments. Ion **40** of *m/z* 499 dissociated by the loss of neutral butene to yield the hydride Te complex of *m/z* 443 and then by loss of phenylacetylene. The intermediate **41** of *m/z* 627 decomposed mainly by neutral loss of Cl–Pd–CH=CHPh to form an ion of *m/z* 327, which dissociated further by sequential loss of HC1 (**36H**$^+$ of *m/z* 291) and butane (*m/z* 233). The ion **39** of *m/z* 717 showed characteristic CID pathways: loss of neutral **36** (PhCH=CHTeBu) gave an ion of *m/z* 431. The ion of *m/z* 499 further dissociated to an ion of *m/z* 341. Herein, by ESI fishing of **39** and **40** in their cationic forms was suggested to exist a solution equilibrium between these two species in the palladium insertion process. It was also suggested BuTeCl to act as a ligand that could stabilize **39**, which may be formed by coordination of two styryl butyl tellurides to $PdCl_2$ followed by transmetalation. Since the relative intensity of the cationic **39** and **40** remained nearly constant during up to 36 h of reaction, as shown by continuous ESI-MS monitoring, the ligand exchange equilibrium between **39** and **40** is likely dynamic. The mechanism in which the cationic **41** is formed was not so straightforwardly rationalized, but a proposed route to **41** involves **40** in a ligand exchange process: that was, exchanged of **36** by [**36** + Bu]$^+$ and further association with neutral HC1 present in the reaction medium. The species **39** and **40** are Pd–styryl complexes that can undergo β-hydrogen elimination to yield PhC≡CH. However, this acetylene was not observed as a byproduct in the coupling reaction. It is known that cations such as Li^+, Ag^+, and Tl^+ can inhibit such β-hydrogen eliminations [58]. It is also known that cation association (**40** → **41**) enhances the solubility of metal complexes [59]. Organocopper cluster intermediates were also identified by ESI-MS and characterized as alkynylcopper species by characteristic Cu isotopic patterns and ESI-MS/MS structural analysis. An expanded catalytic cycle for the coupling of vinylic tellurides with alkynes catalyzed by palladium dichloride was proposed as depicted in Scheme 14.

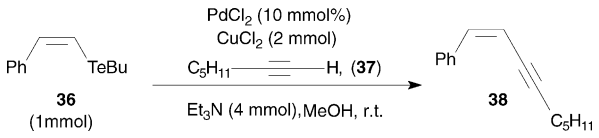

Scheme 13. Coupling of vinylic tellurides with alkynes catalyzed by $PdCl_2$ and $CuCl_2$.

6.2. Heck reaction

The Heck arylation with arenediazonium salts was studied by Eberlin and co-workers through ESI-MS tandem mass spectrometry experiments. The group detected and structurally characterized the main cationic intermediates of this catalytic cycle directly from solution to the gas phase [60]. They proposed a detailed catalytic cycle of the Heck reaction with arene diazonium salts on the basis of the results obtained from ESI experiments using alkene **42** as example, as depicted in Scheme 15.

Roglans and co-workers [61,62] also studied the Heck reaction of arene diazonium salts using a palladium(0) complexes of 15-membered macrocyclic triolefines.

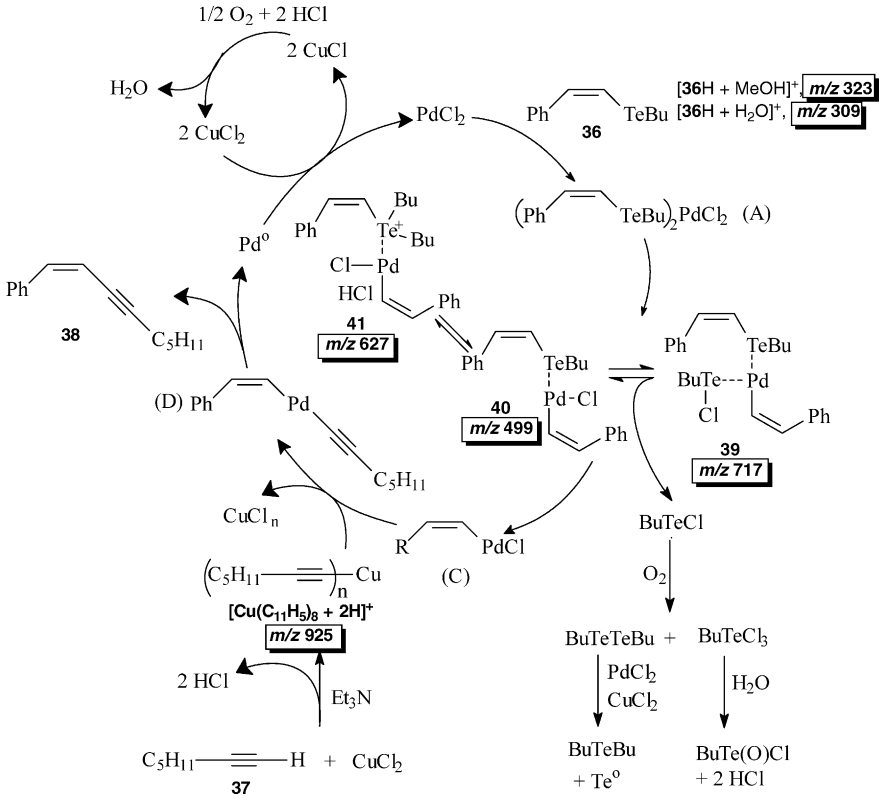

Scheme 14. Expanded mechanism based on ESI(+)-MS tandem MS/MS experiments for the reaction of **36** (0.1 mmol L^{-1}) with alkyne **37** (0.11 $mmol^{-1}$ to give **38** using $PdCl_2$ (0.01 $mmol^{-1}$) and $CuCl_2$ (0.2 $mmol^{-1}$) in the absence of an inert atmosphere.

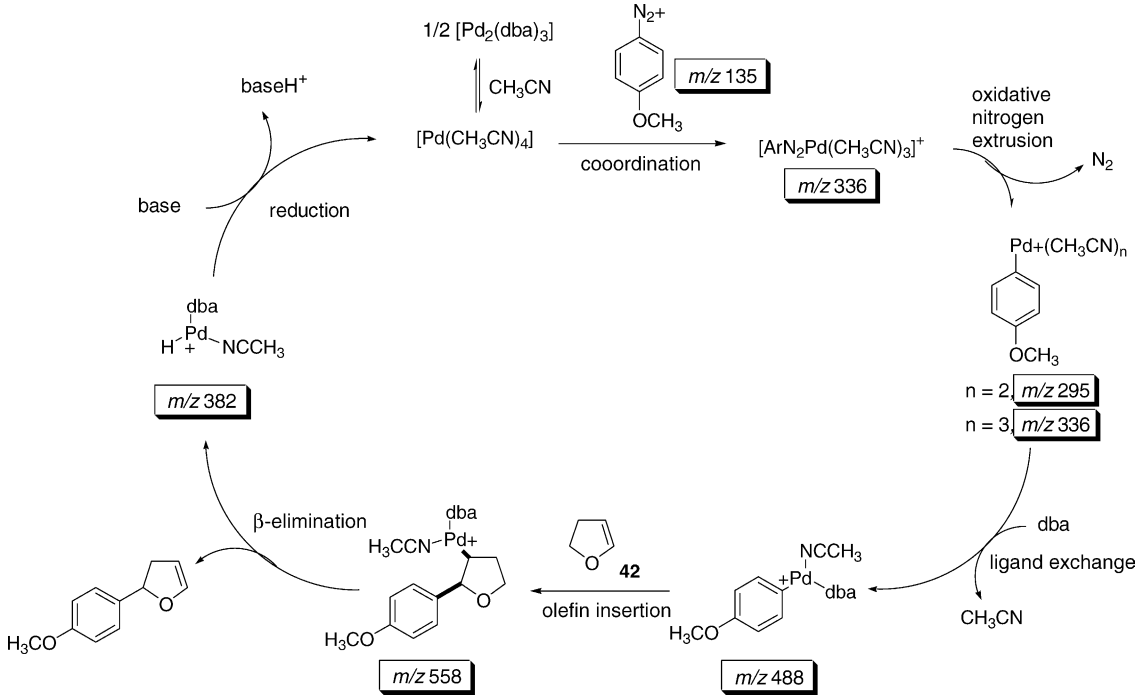

Scheme 15. Proposed catalytic cycle of the Heck reaction with arene diazonium salts.

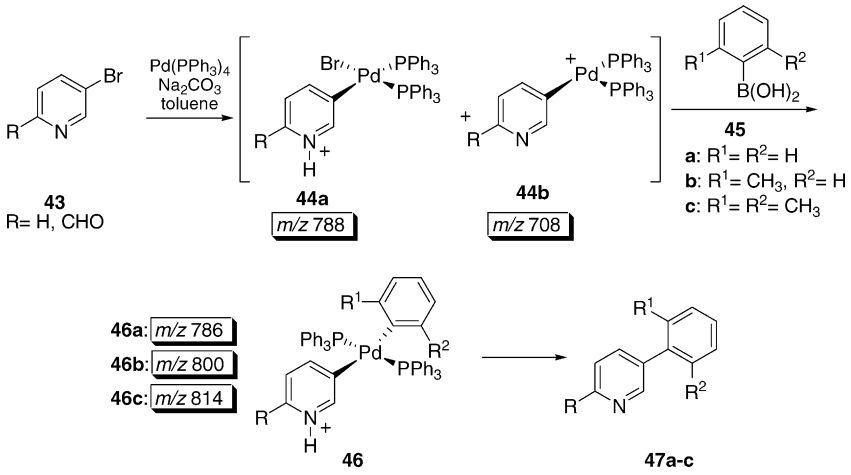

Scheme 16. Pd-catalyzed reaction (0.27 μmol L^{-1}) of pyridyl halides **43** (8.9 μmol L^{-1}) with phenylboronic acids **45a–c** (5.48 μmol L^{-1}) after dilution with MeOH for analysis.

6.3. Suzuki reaction

The Suzuki coupling reaction of pyridyl halide **43** with phenylboronic acids **45a–c** was studied by Aliprantis and Canary (Scheme 16) [25]. They performed off-line ESI-MS investigation, identifying pyridylpalladium(II) complexes as the cation species $[(pyrH)Pd(PPh_3)_2Br]^+$ (**44a**) and $[(pyr)Pd(PPh_3)_2]^+$ (**44b**). Additionally, diarylPd(II) $[(pyrH)(R^1R^2C_6H_3)Pd(PPh_3)_2]^+$ (**46**) and arylPd(II) $[(R^1R^2C_6H_3)Pd(PPh_3)_2]^+$ were observed in the ESI mass spectra. Few years later, some new results were published by Roglans and co-workers on ESI-MS investigation of Pd-catalyzed self-coupling reaction of areneboronic acids [26,63].

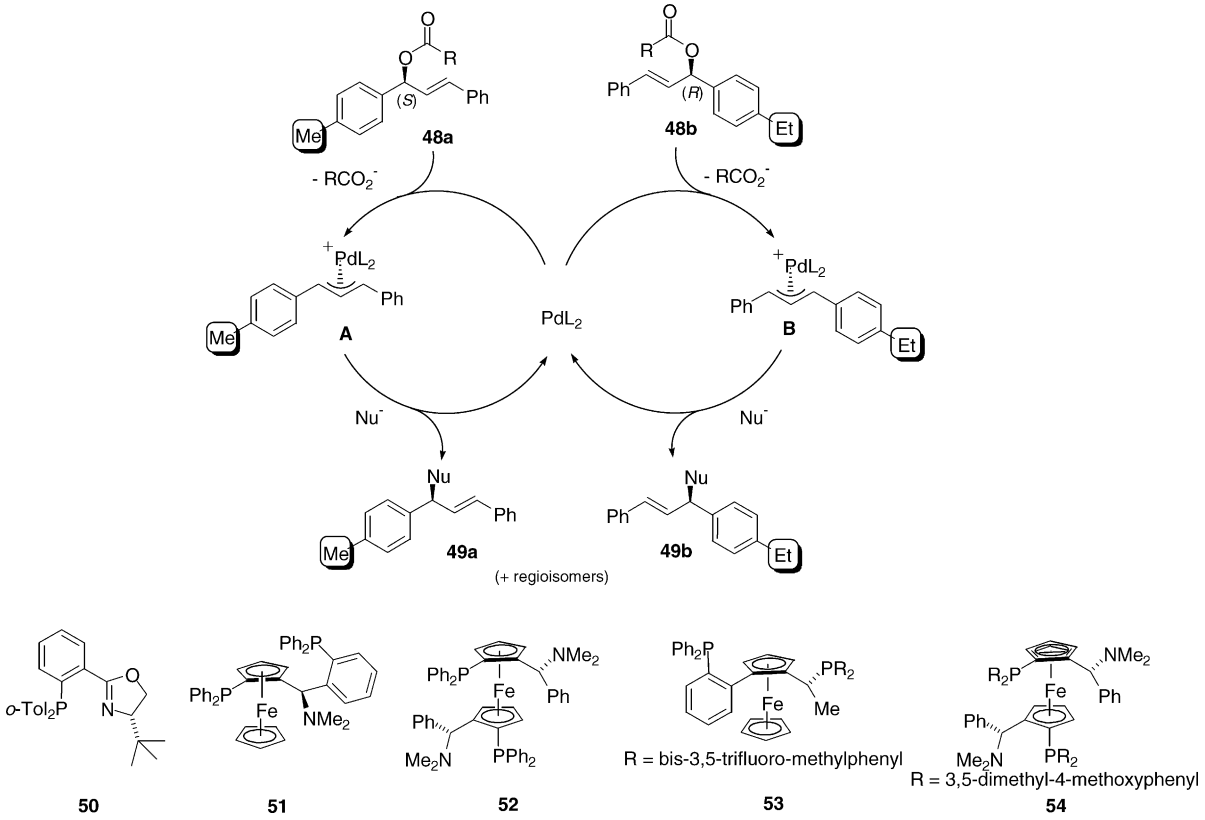

Scheme 17. Simultaneous screening of a mixture of five Pd catalysts (0.1 mmol L^{-1}) performed by Pfaltz. Compounds **48a**,**b** were used as pseudoracemates in solution as inferred by authors that methyl and ethyl groups afforded no great differences in the reactivity of allyl groups toward Pd species, supposing almost the same reactivity behavior for both.

6.4. Allylic substitution reaction

Markert and Pfaltz [64] applied ESI-MS technique for parallel screening of Pd-catalyzed enantioselective allylation reaction of diethyl ethyl malonate with allylic esters. Enantiodiscrimination of a palladium catalyst with different chiral ligands was studied by ESI-MS. In the catalytic cycle proposed (Scheme 17), the first step is the formation of Pd–allyl complexes **A** and **B** is fast, while the second step, nucleophilic addition to the allylic system to give products **49a** and **49b**, is slower. The cationic intermediates **A** and **B** were observed in the ESI-MS spectra. The ratio **A**:**B** was inferred as the catalyst ability to discriminate between two enantiomers with two different alkyl groups at the para position of the aryl group (Ar = 4-methylphenyl in **48a** and 4-ethylphenyl in **48b**). Five different catalyst precursors were tested with different stereoselectivity in homogeneous solution containing pseudoracemate **48a**,**b** and the anion of diethyl ethyl malonate as nucleophiles. All the 10 Pd–allyl intermediates were observed in the ESI-MS screening after 2 min of reactional time. A selectivity order was proposed from the ion intensities ratio based on the ligand as **53** > **52** > **51** ≅ **50** ≅ **54**, being the complex with ligand **53** the most selective catalyst. The group proposed that the technique may be used with unlimited number of catalysts in the screening simultaneously, as long as the signals do not overlap.

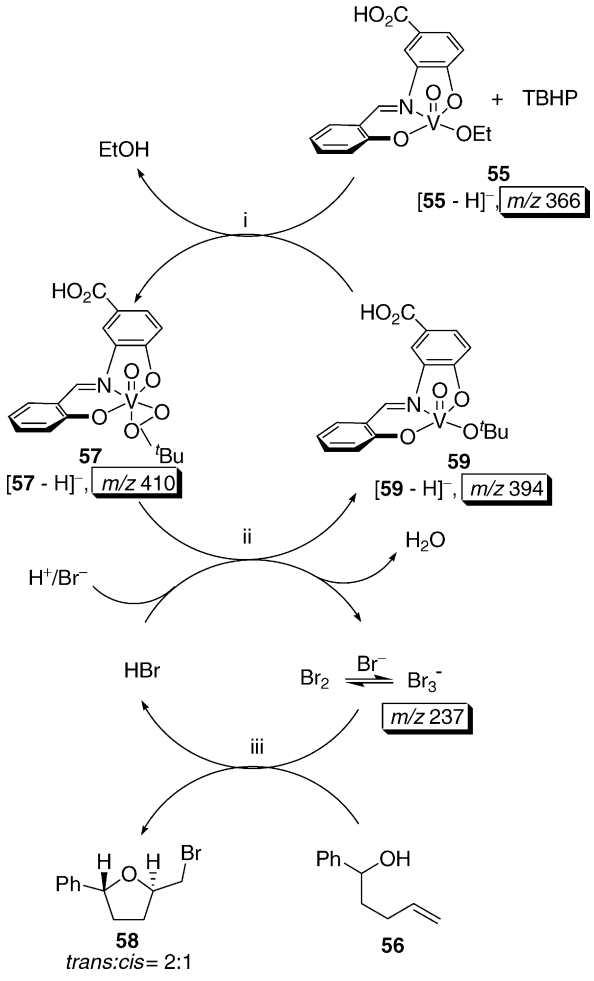

Scheme 18. Schematic presentation of reaction cycles leading to the formation of 2-(bromomethyl)-5-phenyltetrahydrofuran (**58**) from TBHP, pyHBr, l-phenyl-4-penten-l-ol (**56**), via vanadium(V) compounds **57** and **59**. The solutions were diluted with CH_3CN before analysis to a final concentration of 1.0 mmol L^{-1}.

Roglans and co-workers [65] also studied the substitution of allyl acetate by acetylacetone in presence and absence of Pd catalyst by ESI-MS.

6.5. Lewis-catalyzed additions

Ricci and co-workers [66] studied oxazoline moiety fused with a cyclopenta[β]thiophene as ligands on the copper-catalyzed enantioselective addition of Et_2Zn to chalcone. The structure of the active Cu species was determined by ESI-MS. Evans et al. [67] studied C_2-symmetric copper(II) complexes as chiral Lewis acids. The catalyst-substrate species were probed using electrospray ionization mass spectrometry. Comelles and et al. studied Cu(II)-catalyzed Michael additions of β-dicarbonyl compounds to 2-butenone in neutral media [68]. ESI-MS studies suggested that copper enolates of the α-dicarbonyl formed in situ are the active nucleophilic species. Schwarz and co-workers investigated by ESI-MS iron enolates formed in solutions of iron(III) salts and β-ketoesters [69]. Studying the mechanism of palladium complex-catalyzed enantioselective Mannich-type reactions, Fujii et al. characterized a novel binuclear palladium enolate complex as intermediate by ESI-MS [70].

6.6. C–H activation and hydrogenations

Chen and Gerdes [71] performed a combination of ESI-MS and kinetic studies in the Pt^{II}-catalyzed H/D exchange, and Ir-based hydrogenations [72]. Noyori used ESI(+)-MS to intercept the active species of the asymmetric hydrogenation reaction of

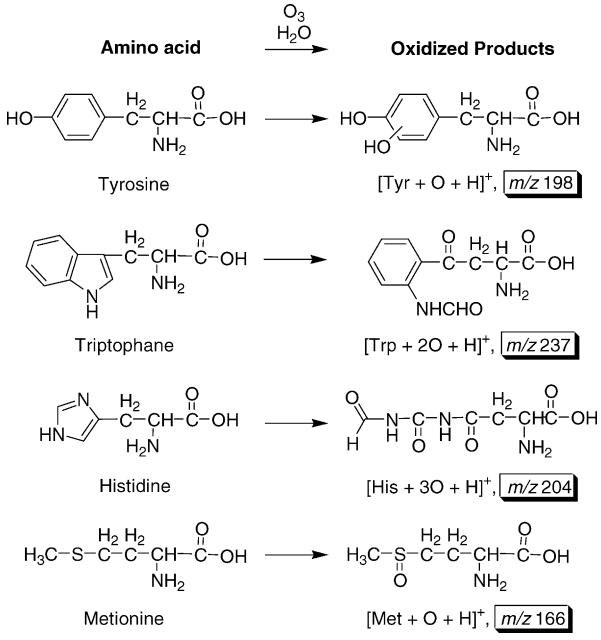

Scheme 19. Ozone oxidation products of amino acids screened by ESI(+)-MS.

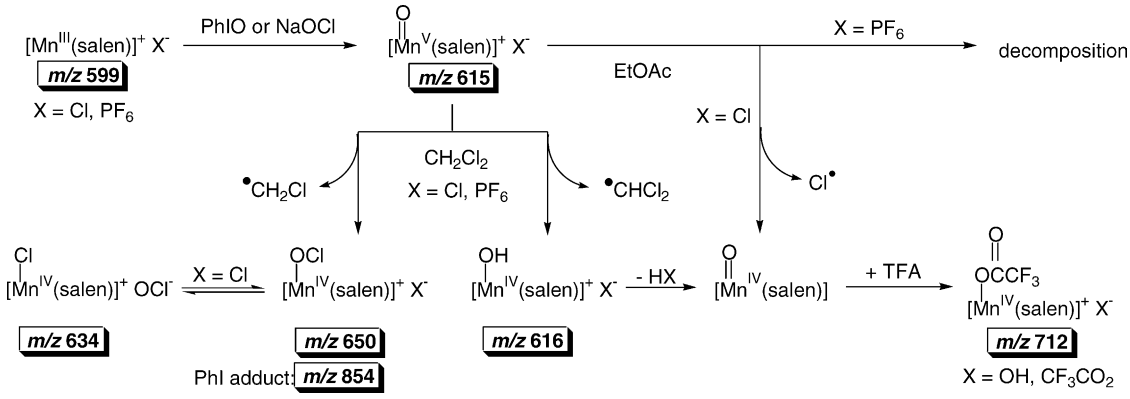

Scheme 20. Mechanism proposed for formation of the various Mn^{IV} complexes.

acetophenone with chiral Ru-complex to give (*R*)-phenylethanol in 82%*ee* [73].

6.7. Oxidations

The (Schiff base)vanadium(V) complex **55** with tridentate imine auxiliaries acts as catalyst for the oxidation of Br^- with *tert*-butyl hydroperoxide (TBHP) in non-aqueous solvents. The principal objective of this study performed by Hartung and co-workers [74] was associated with the search for an adequate combination of bromide source and primary oxidant that would reduce the inherent propensity of (Schiff base)vanadium(V) complexes in the presence of *tert*-butyl hydroperoxide (TBHP) to convert alkenols (**56**) directly into hydroxy-functionalized tetrahydrofurans (**58**) [75]. Reactivity-selectivity studies on the vanadium(V)-catalyzed oxidation of bromide were investigated through ESI(−)-MS^n in order to interpret crucial steps in the process such as peroxide activation and the generation of an active brominating reagent. The reactivity of *tert*-butylperoxy complex **57** was explored by ESI-MS analysis of solutions that were obtained by mixing (Schiff base)vanadium(V) complex **55** in CH_2Cl_2/CH_3CN with TBHP and py-HBr, and an intense ion of *m*/*z* 237 was observed in the negative ion mode, and assigned as Br_3^- ion. Further ions detected in this experiments originated from $[VOL_8(OH)–H]^-$ (*m*/*z* 338), $[VOL_8(Br)_2]^-$ (*m*/*z* 480), and $[V_2O_3(L_8)_2Br]^-$ (*m*/*z* 739). In the positive ion mode ESI spectrum of this sample pointed to the formation of the following cations: $[Py_2H_2Br]^+$ of *m*/*z* 239, $[VOL_8py]^+$ of *m*/*z* 401, $[V_2O_3(L_8)_2H]^+$ of *m*/*z* 661, and $[V_2O_3(L_8)_2pyH]^+$ of *m*/*z* 740. It should, however, be noted that these cations were also detected from a solution of **55** and pyHBr in CH_2Cl_2/CH_3CN without TBHP.

The authors proposed the mechanism of the new method for bromocyclization of alkenols proceeding in three decisive steps as depicted in Scheme 18. In the first step, TBHP binds to a vanadium(V)-based catalyst to furnish the corresponding (*tert*-

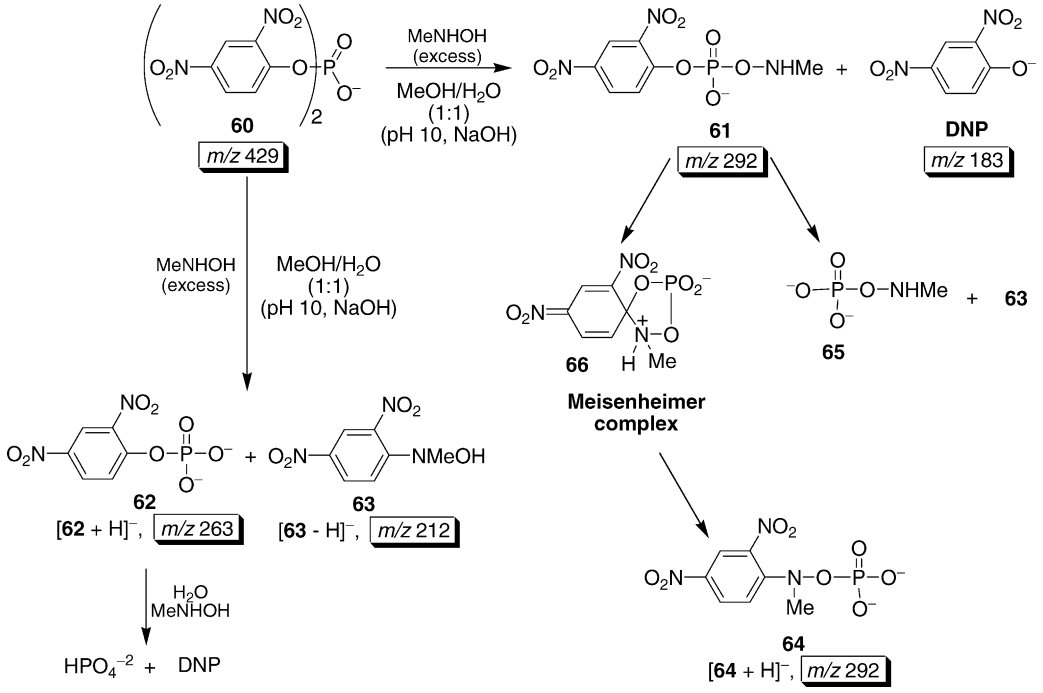

Scheme 21. Mechanism for the reaction of MeNHOH and **60** probed by ESI(−)-MS experiments, which corroborated kinetics studies.

butylperoxy)(Schiff base)vanadium(V) complex (e.g., **57**). The activated peroxide is considered to be the oxidant for the conversion of Br^- into Br_2, which then serves as a brominating reagent for the subsequent bromocyclization of alkenols in a third vanadium(V)-independent step.

Smith and co-workers [76] studied the system l,4,7-trimethyl-l,4,7-triazacyclononane (TMTACN), $MnSO_4$ and H_2O_2, in basic aqueous acetonitrile, and reported it was an effective system for the epoxidation of cinnamic acid. They used ESI(+)-MS to detect the manganese complexes, ligand and ligand oxidation products, and ESI(−)-MS to detect also the substrates and their oxidation products.

Itoh and co-workers [77] used ESI to identify a diiron complex of binaphtol-containing chiral ligand in the catalytic oxidation of alkane with *m*-CPBA to the corresponding alcohols. O'Hair and co-workers [78] reported an example that involves the oxidation of methanol to formaldehyde in the gas phase using binuclear molybdenum oxides, $[Mo_2O_6(OH)]^-$ and $[Mo_2O_5(OH)]^-$, as catalysts and nitromethane as the oxidant.

Aqueous ozonation of the 22 most common amino acids and some small peptides were studied through electrospray mass (ESI-MS) and tandem mass spectrometry by Eberlin and co-workers [79]. After 5 min of ozonation only histidine, metionine, triptamine, and tyrosine formed oxidation products clearly detectable by ESI-MS (Scheme 19).

6.8. Epoxidation

One of the most elegant methods for the selective formation of C–O bonds is the catalytic Jacobsen-Katsuki epoxidation, the enantioselective synthesis of optically active epoxides by oxygen-transfer reactions with chiral, non-racemic manganese oxo salen complexes. These complexes have been suggested as the catalytically active species in epoxidations catalyzed by metal–salen and porphyrin complexes [80]. One of these complexes was for the first time isolated and characterized by Feichtinger and Plattner through ESI-MS studies [81].

Adam et al. have characterized $[Mn^{IV}(salen)]$ complexes by ESI-MS/MS [82]. The group proposed that *cis*- and *trans*-epoxide formation followed separate pathways, and the possibility that the reaction mixture had multiple, rapidly equilibrating oxidizing species, each of which preferentially followed one of the reaction pathways could not be excluded. Herein, they suggested a bifurcation step in the catalytic cycle to account for the dependence of the diastereoselectivities on the oxygen source as depicted in Scheme 20 [82b].

7. Miscellaneous

7.1. Nucleophilic substitution reactions

Eberlin and co-workers [83] have probed the mechanism of nucleophilic substitution reactions of methylated hydroxylamines, hydrazine and hydrogen peroxide with *bis*(2,4-dinitrophenyl)phosphate (BDNPP). The group used ESI-MS in the screening of the reaction by fishing ionic intermediates and products directly from solution into the gas phase, and the key intermediates were fully characterized by ESI-MS/MS experiments. Based on the ESI-MS(/MS) results, NMR and kinetic data, and the results on the reaction of NH_2OH with BDNPP, it was concluded that there was both aromatic substitution, generating DNPP, **62**, and **63**, and initial phosphorylation of the OH group of NHMeOH by BDNPP (Scheme 21, Fig. 9). The latest generates dinitrophenyl oxide (DNP), forming intermediate **61**, which breaks down slowly by two distinct pathways: (a) aromatic nucleophilic substitution described above, giving **63** and **65**, or (b) spontaneous rearrangement where the terminal NHMe group attacks the dinitrophenyl moiety to form a transient cyclic Meisenheimer complex **66**, as for reaction with NH_2OH [84]. This complex **66** rapidly ring opens, giving **64** as a long-lived

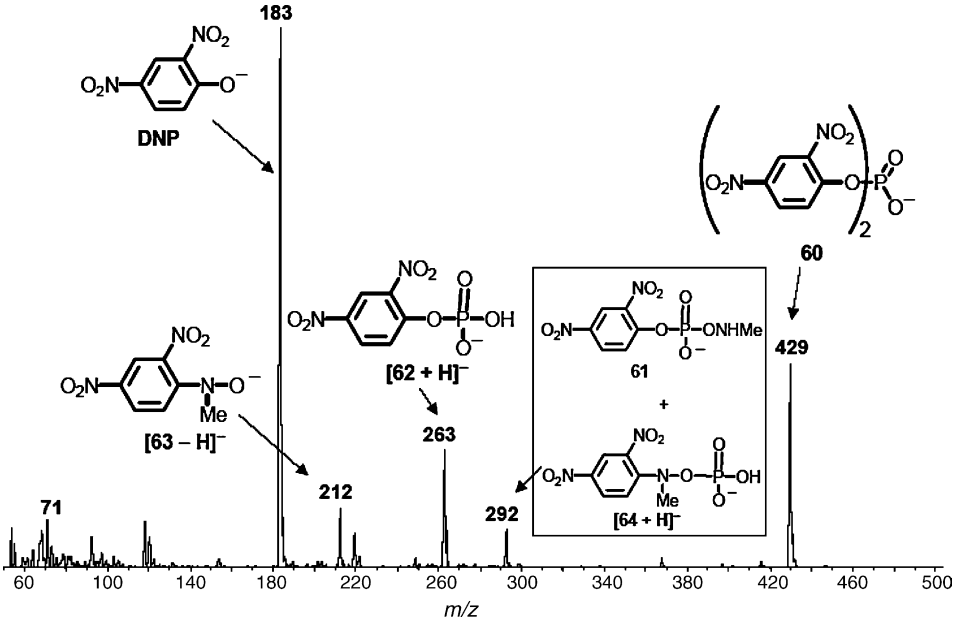

Fig. 9. ESI-MS spectrum of the reaction mixture of 0.01 mol L^{-1} BDNPP with 0.1 mol L^{-1} NHMeOH, in aqueous methanol (50%, v/v) at pH 10.

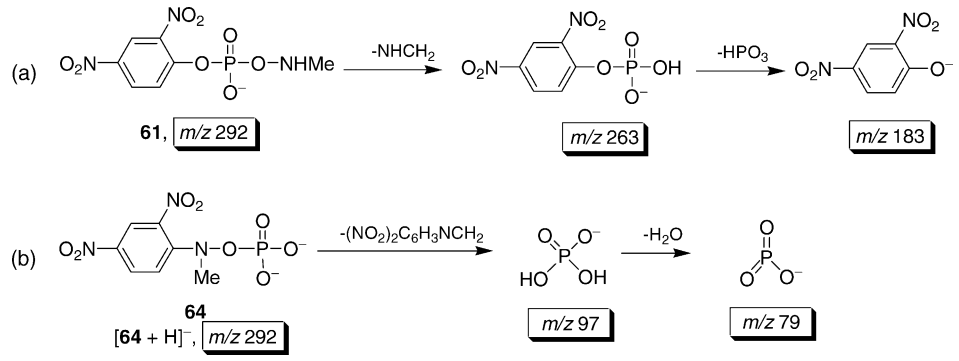

Scheme 22. Differentiation of the isomers **61** (a) and **64** (b) by fragmentation pathways (MS/MS experiments). The isomer **61** (*m*/*z* 292) was proposed to achieve **64** (*m*/*z* 292) through a Meisenheimer complex intermediate.

product as through a mechanism proposed in Scheme 21. Ionic intermediates **61** and **64** (Scheme 21) are isomers, and their relative amounts and therefore the ESI-MS/MS of the ions of *m*/*z* 292 changed drastically with time. Samples taken after 10 min of reaction in solution (Scheme 22(a)) showed that these ions dissociated in the mass spectrometer by CID mainly into four fragment ions of *m*/*z* 263, 183, 97, and 79. The fragment ions, of *m*/*z* 263 and 183, were formed in the gas phase from **61** (Scheme 22(a)), whereas, dissociation to ions of *m*/*z* 97 and 79 was evidence for the presence of **64** (Scheme 22(b)). Therefore, both **61** and **64** were present in the reaction mixture at an early stage of the reaction. After 30 or 60 min of reaction, however, the ion of *m*/*z* 292 generated only the two fragment ions of *m*/*z* 97 and 79. This temporal change in product ion distribution from the CID of ion of *m*/*z* 292 confirmed that in a later stage of reaction intermediate **64**, rather than **61**, became a dominant species through rearrangement from **61** in solution.

8. Conclusion

Over the past few years, there has been a rapid increase in the application of API-MS techniques to the study of organic reaction mechanisms, mainly to intercept for the first time reactive intermediates from these reactions. The ability to isolate ions direct from crude reaction mixtures displays a variety of outstanding features and advantages that allows new applications in mechanistic chemistry of transient species, and undoubtedly API-MS appears as an important tool in the future for studies of labile and sensitive intermediaries in solution, with no need for previous purifications, nor isolation for further characterization of active species, intermediates of reactions, and products due to on-line purifications. Such new MS techniques are also beginning to be used to probe mechanisms of reactions of fundamental importance and practical applications to transfer the reaction intermediates directly from solution to the gas phase. Furthermore, using API-MS many intermediates were intercepted, isolated, detected, and then structurally characterized. We visualize on-line high throughput screening of catalysts applying API mass spectrometry as the next frontier in chemistry that will be developed in few years to be applied on the bench studies as a fast screening method, with MS identification, for a variety of compounds and is likely to find applications in many areas, most particularly in organic synthesis screening and searching for new catalysts.

References

[1] (a) C.M. Whitehouse, R.N. Dreyer, M. Yamashita, J.B. Fenn, Anal. Chem. 57 (1985) 675;
(b) J.B. Fenn, M. Mann, C.K. Meng, S.F. Wong, C.M. Whitehouse, Science 246 (1989) 64;
(c) R.B. Cole (Ed.), Electrospray Ionization Mass Spectrometry—Fundamentals, Instrumentation, and Applications, Wiley, New York, 1997;
(d) J.B. Fenn, J. Am. Soc. Mass Spectrom. 4 (1993) 524.
[2] E.C. Horning, D.I. Carroll, I. Dzidic, K.D. Haegele, M.G. Horning, R.N. Stillwell, J. Chromatogr. Sci. 12 (1974) 725.
[3] (a) D.B. Robb, T.R. Covey, A.P. Bruins, Anal. Chem. 72 (2000) 3653;
(b) T.J. Kauppila, T. Kuuranne, E.C. Meurer, M.N. Eberlin, T. Kotiaho, R. Kostiainen, Anal. Chem. 74 (2002) 5470.
[4] The term “electrospray ionization” must be understood as the technique and not as the ionization process. Electrospray is not an ionization process in the sense that applies, for example, to electron ionization where the process explicitly concerns the conversion of neutral molecules into ions, except in a small minority of examples;
(a) G.J. Van Berkel, S.A. McLuckey, G.L. Glish, Anal. Chem. 64 (1992) 1586;
(b) X.M. Xu, S.P. Nolan, R.B. Cole, Anal. Chem. 66 (1994) 119.
[5] C. Adlhart, P. Chen, Helv. Chim. Acta 83 (2000) 2192.
[6] (a) D.A. Plattner, Int. J. Mass Spectrom. 207 (2001) 125;
(b) D.A. Plattner, Top. Curr. Chem. 225 (2003) 153.
[7] (a) D.I. Carroll, I. Dzidic, R.N. Stillwell, K.D. Haegele, E.C. Horning, Anal. Chem. 47 (1975) 2369;
(b) G.J. Van Berkel, Eur. J. Mass Spectrom. 9 (2003) 539.
[8] D. Fabris, Mass Spectrom. Rev. 24 (2005) 30.
[9] G. Diehl, U. Karst, Anal. Bioanal. Chem. 373 (2002) 390.
[10] (a) J.B. Fenn, M. Mann, C.-K. Meng, S.-F. Wong, C.M. Whitehouse, Mass Spectrom. Rev. 9 (1990) 37;
(b) J.B. Fenn, Angew. Chem. Int. Ed. 42 (2003) 3871.
[11] P. Kebarle, L. Tang, Anal. Chem. 65 (1993) 972.
[12] S.J. Gaskell, J. Mass Spectrom. 32 (1997) 677.
[13] Although somewhat modified following ion/molecule reactions in the interface thus are commonly observed as multiply charged species.
[14] J.L. Jones, A.R. Dongré, A. Somogyi, V.H. Wysocki, J. Am. Chem. Soc. 116 (1994) 8368.
[15] Interception of this process may allow the preservation of relatively strong non-covalent interactions of analytical significance.
[16] P. Kebarle, Y. Ho, in: R.B. Cole (Ed.), Electrospray Ionization Mass Spectrometry, Wiley, New York, 1997, pp. 3–63.

[17] J.F. de la Mora, G.J. Van Berckel, C.G. Enke, R.B. Cole, M. Martinez-Sanchez, J.B. Fenn, J. Mass Spectrom. 35 (2000) 939.
[18] G.J. Van Berkel, in: R.B. Cole (Ed.), Electrospray Ionization Mass Spectrometry, Wiley, New York, 1997, pp. 65–105.
[19] K. Zang, D.M. Zimmerman, A. Chung-Phillips, C.J. Cassidy, J. Am. Chem. Soc. 115 (1993) 10812.
[20] A.T. Blades, P. Jayawera, M.G. Ikonomou, P. Kebarle, J. Chem. Phys. 92 (1990) 5900.
[21] L. Gianelli, V. Amendola, L. Fabbrizzi, P. Pallavicini, G.G. Mellerio, Rap. Commun. Mass Spectrom. 15 (2001) 2347.
[22] (a) R.W. Vachet, J.A.R. Hartman, J.H. Callahan, J. Mass Spectrom. 33 (1998) 1209;
(b) R.W. Vachet, J.R. Hartman, J.W. Gertner, J.H. Callahan, Int. J. Mass Spectrom. 204 (2001) 101;
(c) J.R. Hartman, R.W. Vachet, J.H. Callahan, Inorg. Chim. Acta 297 (2000) 79;
(d) J.R. Hartman, R.W. Vachet, W. Pearson, R.J. Wheat, J.H. Callahan, Inorg. Chim. Acta 343 (2003) 119.
[23] (a) A. Schäfer, B. Fischer, H. Paul, R. Bosshard, M. Hesse, M. Viscontini, Helv. Chim. Acta 75 (1992) 1955;
(b) A. Schäfer, H. Paul, B. Fischer, M. Hesse, M. Viscontini, Helv. Chim. Acta 78 (1995) 1763.
[24] S.R. Wilson, J. Perez, A. Pasternak, J. Am. Chem. Soc. 115 (1993) 1994.
[25] A.O. Aliprantis, J.W. Canary, J. Am. Chem. Soc. 116 (1994) 6985.
[26] M. Moreno-Manãs, M. Pérez, R. Pleixats, J. Org. Chem. 61 (1996) 2346.
[27] G. Hambitzer, J. Heitbaum, Anal. Chem. 58 (1986) 1067.
[28] J.W. Sam, X.-J. Tang, R.S. Magliozzo, J. Peisach, J. Am. Chem. Soc. 117 (1995) 1012.
[29] (a) C. Hinderling, P. Chen, Angew. Chem. Int. Ed. 38 (1999) 2253;
(b) C. Hinderling, P. Chen, Int. J. Mass Spectrom. 195 (2000) 377.
[30] P. Chen, Angew. Chem. Int. Ed. 42 (2003) 2832.
[31] J. Griep-Raming, S. Meyer, T. Bruhn, J.O. Metzger, Angew. Chem. Int. Ed. 41 (2002) 2738.
[32] S. Meyer, J.O. Metzger, Anal. Bioanal. Chem. 377 (2003) 1108.
[33] D.J. Wilson, L. Konermann, Anal. Chem. 75 (2003) 6408.
[34] (a) R. Arakawa, L. Jian, A. Yoshimura, K. Nozaki, T. Ohno, H. Doe, T. Matsuo, Inorg. Chem. 34 (1995) 3874;
(b) R. Arakawa, S. Mimura, G. Matsubayashi, T. Matsuo, Inorg. Chem. 35 (1996) 5725.
[35] J. Brum, P. Dell'Orco, Rapid Commun. Mass Spectrom. 12 (1998) 741.
[36] P. Dell'Orco, J. Brum, R. Matsuoka, M. Badlani, K. Muske, Anal Chem. 71 (1999) 5165.
[37] (a) W. Ding, K.A. Johnson, I.J. Amster, C. Kutal, Inorg. Chem. 40 (2001) 6865;
(b) W. Ding, K.A. Johnson, C. Kutal, I.J. Amster, Anal. Chem. 75 (2003) 4624.
[38] A.D. Modestov, J. Gun, I. Savotine, O. Lev, J. Electroanal. Chem. 565 (2004) 7.
[39] S. Meyer, R. Koch, J.O. Metzger, Angew. Chem. Int. Ed. 42 (2003) 4700.
[40] S. Fürmeier, J.O. Metzger, J. Am. Chem. Soc. 126 (2004) 14485.
[41] S. Fürmeier, J. Griep-Raming, A. Hayen, J.O. Metzger, Chem. Eur. J. 11 (2005) 5545.
[42] (a) A. Hayen, R. Koch, J.O. Metzger, Angew. Chem. Int. Ed. 39 (2000) 2758;
(b) A. Hayen, R. Koch, W. Saak, D. Haase, J.O. Metzger, J. Am. Chem. Soc. 112 (2000) 12458.
[43] T.F. Hess, T.S. Renn, R.J. Watts, A.J. Paszczynski, Analyst 128 (2003) 156.
[44] J. Griep-Raming, J.O. Metzger, Anal. Chem. 72 (2000) 5665.
[45] R. Arakawa, S. Tachiyashiki, T. Matsuo, Anal. Chem. 67 (1995) 4133.
[46] R. Arakawa, F. Matsuda, G.-E. Matsubayashi, T. Matsuo, J. Am. Soc. Mass Spectrom. 8 (1997) 713.
[47] K. Kimura, R. Mizutani, M. Yokoyama, R. Arakawa, G.-E. Matsubayashi, M. Okamoto, H. Doe, J. Am. Chem. Soc. 119 (1997) 2062.
[48] R. Arakawa, J. Lu, K. Mizuno, H. Inoue, H. Doe, T. Matsuo, Int. J. Mass Spectrom. Ion Processes 160 (1997) 371.
[49] D.I. Schuster, J.R. Cao, N. Kaprinidis, Y.H. Wu, A.W. Jensen, Q.Y. Lu, H. Wang, S.R. Wilson, J. Am. Chem. Soc. 118 (1996) 5639.
[50] (a) T.P. Gill, K.R. Mann, Inorg. Chem. 22 (1983) 1986;
(b) A.M. McNair, J.L. Schrenk, K.R. Mann, Inorg. Chem. 23 (1984) 2633;
(c) D.R. Chrisope, K.M. Park, G.B. Schuster, J. Am. Chem. Soc. 111 (1989) 6195;
(d) V. Jakubek, A.J. Lees, Inorg. Chem. 39 (2000) 5779.
[51] S.P. Keizer, W.J. Han, M.J. Stillman, Inorg. Chem. 41 (2002) 353.
[52] L.S. Santos, C.H. Pavam, W.P. Almeida, F. Coelho, M.N. Eberlin, Angew. Chem. Int. Ed. 43 (2004) 4330.
[53] (a) J.S. Hill, N.S. Isaacs, J. Phys. Org. Chem. 3 (1990) 285;
(b) H.M.R. Hoffmann, J. Rabe, Angew. Chem. Int. Ed. 22 (1983) 796;
(c) M.L. Bode, P.T. Kaye, Tetrahedron Lett. 32 (1991) 5611;
(d) Y. Fort, M.-C. Berthe, P. Caubere, Tetrahedron 48 (1992) 6371.
[54] H.M.C. Ferraz, F.L.C. Pereira, E.R.S. Gonçalo, L.S. Santos, M.N. Eberlin, J. Org. Chem. 70 (2005) 110.
[55] C. Raminelli, M.H.G. Prechtl, L.S. Santos, M.N. Eberlin, J.V. Comasseto, Organometallics 23 (2004) 3990.
[56] They also monitored the reaction with ESI-MS in the negative ion mode, but no metal anions were detected.
[57] (a) L. Ripa, A. Hallberg, J. Org. Chem. 61 (1996) 7147;
(b) J.M. Brown, K.K. Hii, Angew. Chem. Int. Ed. 35 (1996) 657;
(c) K.K. Hii, T.D.W. Claridge, J.M. Brown, Angew. Chem. Int. Ed. 36 (1997) 984.
[58] (a) Z. Wang, Z.G. Zhang, X.Y. Lu, Organometallics 19 (2000) 775;
(b) Z.G. Zhang, X.Y. Lu, Q.H. Zang, X.L. Han, Organometallics 20 (2001) 3724;
(c) G.S. Liu, X.Y. Lu, Tetrahedron Lett. 43 (2002) 6791;
(d) A. de Meijere, F.E. Meyer, Angew. Chem. Int. Ed. 33 (1994) 2379 (and references therein).
[59] A. Alexakis, J. Berlan, Y. Besace, Tetrahedron Lett. 27 (1986) 1047.
[60] A.A. Sabino, A.H.L. Machado, C.R.D. Correia, M.N. Eberlin, Angew. Chem. Int. Ed. 43 (2004) 2514.
[61] J. Masllorens, M. Moreno-Manãs, A. Pla-Quintana, A. Roglans, Org. Lett. 5 (2003) 1559.
[62] M. Moreno-Manãs, R. Pleixats, R.M. Sebastian, A. Vallribera, A. Roglans, J. Organomet. Chem. 689 (2004) 3669.
[63] M.A. Armendia, F. Lafont, M. Moreno-Manãs, R. Pleixats, A. Roglans, J. Org. Chem. 64 (1999) 3592.
[64] C. Markert, A. Pfaltz, Angew. Chem. Int. Ed. 43 (2004) 2498.
[65] C. Chevrin, J. Le Bras, F. Hénin, J. Muzart, A. Pla-Quintana, A. Roglans, R. Pleixats, Organometallics 23 (2004) 4796.
[66] B.F. Bonini, E. Capitò, M. Comes-Franchini, A. Ricci, A. Bottoni, F. Bernardi, G.P. Miscione, L. Giordano, A.R. Cowley, Eur. J. Org. Chem. (2004) 4442.
[67] D.A. Evans, M.C. Kozlowski, J.A. Murry, C.S. Burgey, K.R. Campos, B.T. Connell, R.J. Staples, J. Am. Chem. Soc. 121 (1999) 669.
[68] J. Comelles, M. Moreno-Manãs, E. Perez, A. Roglans, R.M. Sebastian, A. Vallribera, J. Org. Chem. 69 (2004) 6834.
[69] C. Trage, D. Schröder, H. Schwarz, Chem. Eur. J. 11 (2005) 619.
[70] A. Fujii, E. Hagiwara, M. Sodeoka, J. Am. Chem. Soc. 121 (1999) 5450.
[71] (a) G. Gerdes, P. Chen, Organometallics 22 (2003) 2217;
(b) G. Gerdes, P. Chen, Organometallics 23 (2004) 3031.
[72] (a) C. Hinderling, D.A. Plattner, P. Chen, Angew. Chem. Int. Ed. 36 (1997) 243;
(b) C. Hinderling, D. Feichtinger, D.A. Plattner, P. Chen, J. Am. Chem. Soc. 119 (1997) 10793;
(c) R. Dietiker, P. Chen, Angew. Chem. Int. Ed. 43 (2004) 5513.
[73] C.A. Sandoval, T. Ohkuma, K. Muniz, R. Noyori, J. Am. Chem. Soc. 125 (2003) 13490.
[74] M. Greb, J. Hartung, F. Köhler, K. Spehar, R. Kluge, R. Csuk, Eur. J. Org. Chem. (2004) 3799.
[75] (a) J. Hartung, M. Greb, J. Organomet. Chem. 661 (2002) 67;
(b) J. Hartung, S. Drees, M. Greb, P. Schmidt, I. Svoboda, H. Fuess, A. Murso, D. Stalke, Eur. J. Org. Chem. (2003) 2388.

[76] B.C. Gilbert, J.R.L. Smith, A.M.I. Payeras, J. Oakes, R.P.I. Prats, J. Mol. Catal. A: Chem. 219 (2004) 265.
[77] T. Nagataki, Y. Tachi, S. Itoh, J. Mol. Catal. A: Chem. 225 (2005) 103.
[78] T. Waters, R.A.J. O'Hair, A.G. Wedd, Chem. Commun. (2000) 225.
[79] T. Kotiaho, M.N. Eberlin, P. Vainiotalo, R. Kostiainen, J. Am. Soc. Mass Spectrom. 11 (2000) 526.
[80] (a) E.N. Jacobsen, in: I. Ojima (Ed.), Catalytic Asymmetric Synthesis, VCH Publishers, New York, 1993, pp. 159–202;
(b) T. Katsuki, J. Mol. Catal. A: Chem. 113 (1996) 87;
(c) K. Srinivasan, P. Michaud, J.K. Kochi, J. Am. Chem. Soc. 108 (1986) 2309;
(d) T.L. Siddall, N. Miyaura, J.C. Huffman, J.K. Kochi, J. Chem. Soc. Chem. Commun. (1983) 1185;
(e) E.G. Samsel, K. Srinivasan, J.K. Kochi, J. Am. Chem. Soc. 107 (1985) 7606;
(f) K. Srinivasan, J.K. Kochi, Inorg. Chem. 24 (1985) 4671.
[81] D. Feichtinger, D.A. Plattner, Chem. Eur. J. 7 (2001) 591.
[82] (a) W. Adam, C. Mock-Knoblauch, C.R. Saha-Moller, M. Herderich, J. Am. Chem. Soc. 122 (2000) 9685;
(b) W. Adam, K.J. Roschmann, C.R. Saha-Moller, D. Seebach, J. Am. Chem. Soc. 124 (2002) 5068.
[83] (a) J.B. Domingos, E. Longhinotti, T.A.S. Brandão, C.A. Bunton, L.S. Santos, M.N. Eberlin, F. Nome, J. Org. Chem. 69 (2004) 6024;
(b) J.B. Domingos, E. Longhinotti, T.A.S. Brandão, L.S. Santos, M.N. Eberlin, C.A. Bunton, F. Nome, J. Org. Chem. 69 (2004) 7898.
[84] J.B. Domingos, E. Longhinotti, C.A. Bunton, F. Nome, J. Org. Chem. 68 (2003) 7051.